



Title	Study of haze-komi and metabolite distribution relation in rice koji by the combination of metabolomics and imaging techniques
Author(s)	Wisman, Putri Adinda
Citation	大阪大学, 2021, 博士論文
Version Type	VoR
URL	<a href="https://doi.org/10.18910/82198">https://doi.org/10.18910/82198</a>
rights	
Note	

*The University of Osaka Institutional Knowledge Archive : OUKA*

<https://ir.library.osaka-u.ac.jp/>

The University of Osaka

# **Doctoral Dissertation**

## **Study of *haze-komi* and metabolite distribution relation in rice *koji* by the combination of metabolomics and imaging techniques**

Adinda Putri Wisman

January 2021

Biotechnology Global Human Resource Development Program,  
Division of Advanced Science and Biotechnology,  
Graduate School of Engineering,  
Osaka University



## Table of Contents

List of Abbreviations .....	5
Chapter 1 General Introduction .....	6
1.1 Rice <i>koji</i> .....	6
1.2 Histochemical staining by $\beta$ -Glucuronidase (GUS) .....	8
1.3 Metabolite profiling by GC-MS and LC-MS .....	9
1.3.1 General concept .....	9
1.3.2 Application of metabolite profiling for food-related samples.....	11
1.4 Mass spectrometry imaging.....	12
1.4.1 General concept .....	12
1.4.2 Matrix-assisted laser desorption/ionization mass spectrometry imaging .	13
1.4.3 Application of MALDI-MSI for food samples .....	15
1.5 Objective of this study .....	16
1.6 Thesis outline.....	16
Chapter 2 Mapping of <i>haze-komi</i> using GUS staining .....	18
2.1 Introduction .....	18
2.2 Experimental.....	19
2.2.1 <i>Aspergillus oryzae</i> GUS strain construction .....	19
2.2.2 Rice <i>koji</i> making.....	19
2.2.3 Mycelia content estimation .....	20
2.2.4 Rice <i>koji</i> sectioning.....	20
2.2.5 Histochemical staining and observation .....	21
2.3 Results and discussion .....	21
2.3.1 Rice <i>koji</i> sectioning.....	21
2.3.2 Time-course observation of <i>haze-komi</i> in rice <i>koji</i> .....	22

2.4	Conclusion.....	26
Chapter 3 Time-course metabolite profiling of rice <i>koji</i> .....		27
3.1	Introduction .....	27
3.2	Experimental.....	27
3.2.1	Samples and chemicals .....	27
3.2.2	Sample extraction for GC-MS and LC-MS analysis .....	28
3.2.3	Derivatization for GC-MS analysis .....	28
3.2.4	GC-MS analysis.....	29
3.2.5	LC-MS analysis .....	29
3.2.6	Data processing and multivariate analysis .....	29
3.3	Results and discussion .....	30
3.3.1	Time-course metabolite profiling of rice <i>koji</i> .....	30
3.3.2	Changes in sugar and sugar alcohols profile during rice <i>koji</i> -making.....	33
3.3.3	Changes in amino acids profile during rice <i>koji</i> -making .....	36
3.3.4	Changes in other metabolites during rice <i>koji</i> -making .....	38
3.4	Conclusion.....	40
Chapter 4 Visualization of metabolites in rice <i>koji</i> made by GUS strain <i>Aspergillus oryzae</i> .....		41
4.1	Introduction .....	41
4.2	Experimental.....	41
4.2.1	Samples and chemicals .....	41
4.2.2	Sample preparation .....	42
4.2.3	MALDI-IT-TOF MSI analysis .....	42
4.3	Results and discussion .....	43
4.3.1	Mass imaging of sugars and sugar alcohols .....	43
4.3.2	Mass imaging of amino acids .....	46

4.3.3	Mass imaging of other amine metabolites .....	51
4.4	Conclusion.....	53
Chapter 5 Conclusion and Future Perspective.....		54
5.1	Conclusion.....	54
5.2	Future perspective.....	54
References .....		56
List of Publications .....		62
Appendices .....		64
Acknowledgment .....		79

## List of Abbreviations

*(in alphabetical order)*

ACN: Acetonitrile

CMC: Carboxymethyl cellulose

DHB: 2,5-dihydroxybenzoic acid

DPP-TFB: 2,4-diphenyl-pyranylium tetrafluoroborate

GC: Gas Chromatography

GC-MS: Gas Chromatography coupled Mass Spectrometry

GUS:  $\beta$ -Glucuronidase

ITO: Indium Tin Oxide

LC: Liquid Chromatography

LC-MS: Liquid Chromatography coupled Mass Spectrometry

MALDI: Matrix-Assisted Laser Desorption/Ionization

MALDI-IT-TOF: MALDI coupled with Ion Trap and Time-of-Flight Mass Spectrometer

MALDI-MSI: Matrix-Assisted Laser Desorption/Ionization Mass Spectrometry Imaging

MS: Mass Spectrometry

MS/MS: tandem mass spectrometry

MSI: Mass Spectrometry Imaging

MSTFA: N-methyl-N-trimethylsilyl-trifluoroacetamide

$m/z$ : mass-to-charge ratio

NEDC: N-(1-Naphthyl) ethylenediamine dihydrochloride

NRIB: National Research Institute of Brewing

OCT: Optimal Cutting Temperature

PCA: Principal Component Analysis

TEA: Triethylamine

TFA: Trifluoroacetic acid

X-Gluc: 5-bromo-4-chloro-3-indoyl glucuronide

# Chapter 1

## General Introduction

The use of fermentation by fungi for producing foodstuffs has been known for centuries. The nature of the fermentation gives added value to foodstuffs, both in terms of taste and nutrients. Rice *koji* is one of the fungal-inoculated materials that is important for the food and beverage industry. However, the improvement of rice *koji* quality is mainly based on trial and error, since many aspects are still not known regarding the events that occurred during the rice *koji*-making process. Notably, while the profile of mycelial distribution was said to be connected with the metabolite contents of rice *koji* (Ito et al. 1990; Iwano et al. 2002), no previous study was able to correlate them directly. In this thesis, the correlation between degree of mycelial penetration (*haze-komi*) and the amount as well as distribution profile of metabolites was explored through the combination of metabolomics approach and visualization techniques by applying histochemistry staining as well as mass spectrometry imaging.

### 1.1 Rice *koji*

Rice *koji* is a material made from steamed rice inoculated by the *koji* mold *Aspergillus oryzae* (*A. oryzae*). Rice *koji* is involved in the production of various fermented products, such as *sake*, *mirin*, *miso*, and others. Figure 1.1 shows an example of rice *koji*-making procedure for *sake* production. The rice used for *sake* brewery is a special rice grown for *sake*, and the outer part is polished to remove peptides and lipids. The degree of polishing, also referred to as the rice-polishing ratio, is the percentage of white rice left after polishing.

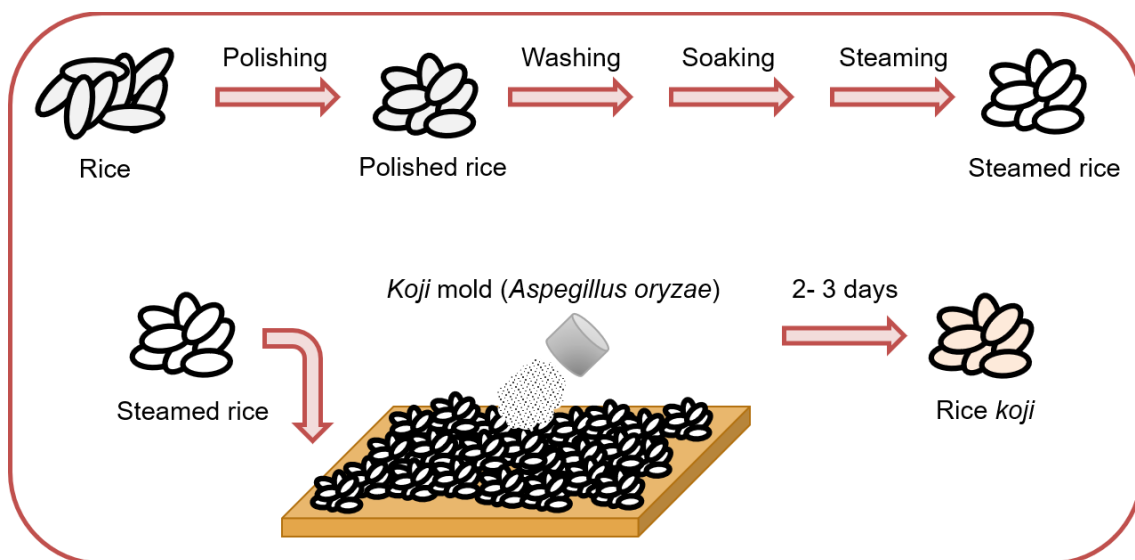


**Figure 1.1 Rice *koji*-making process**

After polishing, rice is then washed, soaked, and finally steamed. The cooled steamed rice was then used as the media for *koji* mold growth. In the traditional method, cooled steamed rice is transported to a special room, where conidial spore of *koji* mold is spread to the steamed rice. The room is kept at around 30°C and humidity maintained in the range of 50% - 80%. Mixing of the grains was done in two- or three-hour intervals for around three days. This procedure promotes *koji* mold to propagate and, as a result, produces enzymes and various metabolites that will be used later in the main fermentation step with yeast (Fujita et al. 2003).

Rice *koji* is considered as an important material that affects the quality of the end products. As such, the examination of rice *koji* features is essential for the overall production process. The activity of amylolytic enzymes and protease inside rice *koji* is the generally measured feature. On the other hand, the appearance of rice *koji* are also examined regularly. White areas called “*haze*” that extend across the surface of the steamed rice becomes the parameter to determine whether the rice *koji* is ready to be used for the next step in production. This white color is believed to be the *A. oryzae* fungi growing on the rice. Figure 1.2 shows an example of a rice *koji* surface covered with *haze*. The fungi also grow into the internal part of steamed rice (Ito et al. 1989). The degree of fungal mycelial penetration is known as *haze-komi*, and it is thought to have a high correlation with the components of rice *koji*.



**Figure 1.2** Surface photo of steamed rice and rice *koji*

## 1.2 Histochemical staining by $\beta$ -Glucuronidase (GUS)

$\beta$ -Glucuronidase (GUS) reporter gene system is a common technique used in plant molecular biology and microbiology since the enzyme has no or low activity in higher plants, fungi, and bacteria. The system utilizes the GUS gene from *Escherichia coli* encoded by the *uidA* locus. Depending on the substrate used, this system can be used for different assays, such as fluorimetric, spectrophotometric, and histochemical assays. The first demonstration of this system was by Jefferson et al on a tobacco plant. The transformed tobacco plant containing *uidA* was subjected to various glucuronide substrates for fluorimetric and histochemical assays.

For histochemical assay, the commonly used substrate is 5-bromo-4-chloro-3-indoyl glucuronide (X-Gluc). The reaction catalyzed by the GUS enzyme will produce a colorless and soluble compound, 5-bromo-4-chloro-3-indoyl. The main product will then undergo oxidation and dimerization, forming 5,5'-dibromo-4,4'-dichloro-indigo that exhibits indigo color for visualization. The full reaction is described in Figure 1.3.

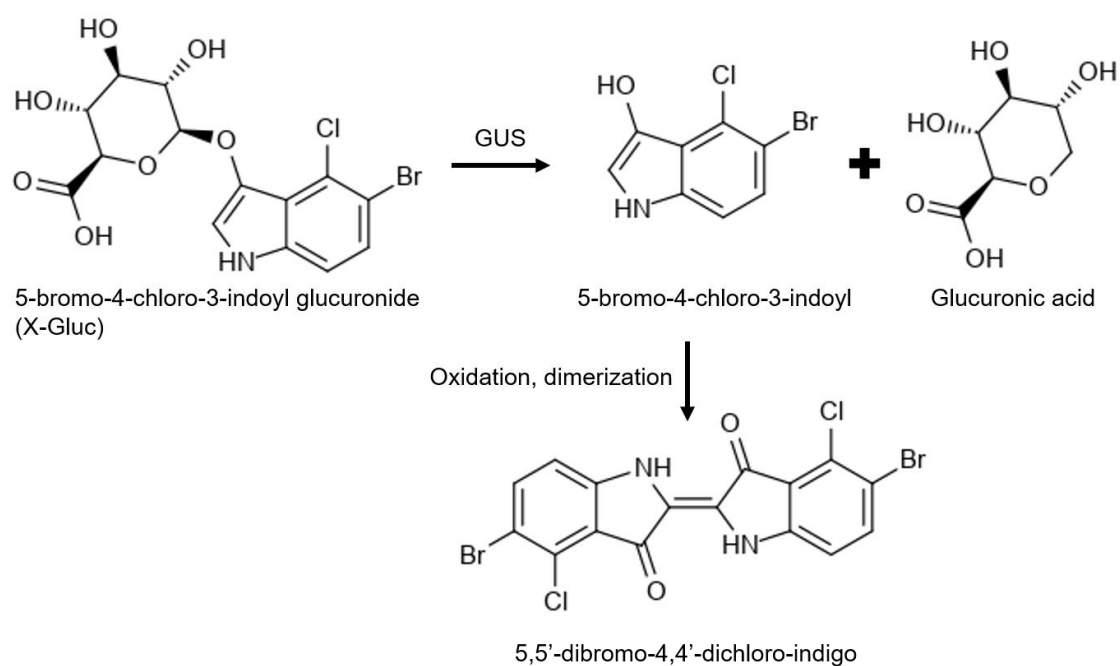


**Figure 1.3 GUS histochemical reaction**

The application of histochemical staining using GUS for fungi has been previously reported. In 1993, Oliver et al reported the use of this system to observe fungal infection of *Cladosporium fulvum* on a tomato leaf. Another study by Brown et al also demonstrated the use of this system to monitor *Aspergillus flavus* growth in maize kernels. These studies demonstrated the usefulness of GUS histochemical staining to observe fungal distribution in solid media.

### 1.3 Metabolite profiling by GC-MS and LC-MS

#### 1.3.1 General concept

Metabolite profiling is an analytical strategy that focuses on a large group of metabolites that are related to a specific metabolic pathway or a class of compounds (Wolfender et al. 2015). Metabolite profiling is often employed to correlate between the observed traits and metabolites comprised in the sample of interest. The levels of detected metabolites are compared between samples, and hypothesis could be generated from the discrimination or grouping of the samples based on the metabolite profile.

Chromatography combined with mass spectrometry analytical methods is often employed to obtain a comprehensive metabolite profile. Chromatography provides separation of compounds based on their chemical properties, while mass spectrometry

(MS) accommodates metabolite detection and mass annotation. Gas Chromatography (GC) is one of the most established platforms for metabolite profiling, especially for non-targeted profiling due to its robustness. On the other hand, Liquid Chromatography (LC) is an emerging technique that provides broader coverage of metabolites because of its flexibility with mobile phase composition and the absence of derivatization step. LC is also especially useful for compounds that are thermally labile and cannot be analyzed by using GC. The general workflow of metabolite profiling by GC-MS and LC-MS can be found in Figure 1.4.

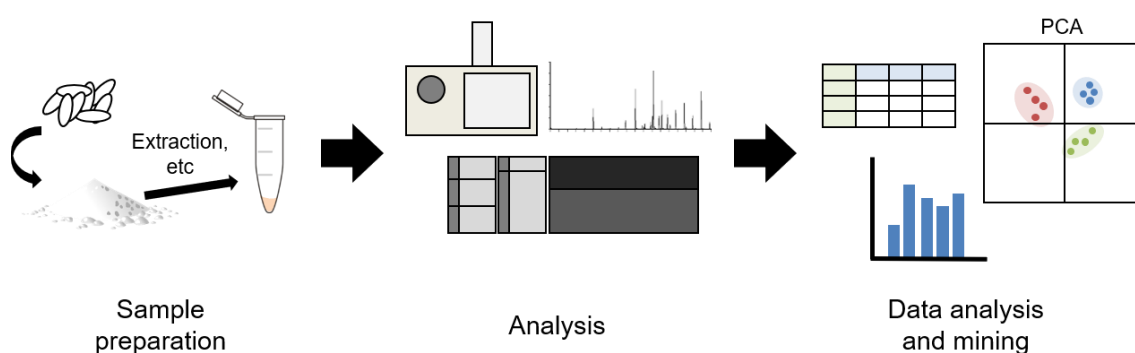


**Figure 1.4 General metabolite profiling workflow**

- **Sample preparation**

Sample preparation is a critical stage for the analysis of metabolites. Depending on the samples used and target analytes, many details are considered in this stage, including during sampling, extraction, and optionally, derivatization process. For solid samples, homogenization into fine powder by milling is required before the extraction step. The solvent used for the extraction of metabolites from the sample is commonly based on the Bligh and Dyer method, which includes a mixture of water, methanol, and chloroform with a certain ratio (Breil et al. 2017). While this method was originally developed for extracting lipid metabolites, the presence of water and methanol enables the extraction of hydrophilic metabolites as well.

Derivatization will chemically modify and transform a specific target structure to improve the detection characteristics of metabolites in GC-MS or LC-MS analysis (Aretz and Meierhofer 2016). Derivatization step is especially required for analysis using GC, as the metabolites need to be volatile to be analyzed in the gas phase. Two-step derivatization step involving oximation and silylation is frequently applied to

comprehensively measure polar molecules such as sugars, amino acids, and organic acids (Halket et al. 2005). Oximation will provide protection for the keto groups and prevent the conversion of sugar chain form into cyclic form, while silylation will replace hydrogen atoms of hydroxyl group, carboxyl group, and amino group in the analytes into silyl group, increasing the stability and volatility of the analytes.

- **Sample analysis**

The selection of mobile and stationary phase should be considered for metabolome analysis using chromatography combined with mass spectrometry. For analysis using GC-MS, inert gases such as hydrogen and helium are used as the carrier gas, while column selection is based on the analytes that will be focused on. The temperature gradient during the analysis can be adjusted for sensitivity improvement. For LC-MS analysis, a diverse selection of both mobile phases composition and columns are available. Analysis of polar metabolites usually employs reversed-phase or hydrophilic interaction (HILIC) separation modes. The elution method based on analysis time can also be modified, improving the separation of analytes in the sample.

- **Data analysis and mining**

First, the detected ions from the mass spectrometer are converted to a scale of intensity, followed by metabolite annotation based on the retention time and mass spectra profile. This allows the creation of a data matrix of the name of each detected metabolite with its intensity in every sample. This data then can be used for simple intensity comparison between samples or further processed by means of multivariate analysis. One of the most commonly used analyses for metabolomics data is principal component analysis (PCA), which is useful for observing trends and clusters within a set of samples.

### **1.3.2 Application of metabolite profiling for food-related samples**

In the field of food study, metabolite profiling is commonly used to understand the effect of various factors that may affect the characteristic of a certain food commodity. The various factors range from natural environmental to man-made, such as in the case of processed food. Metabolomic approach is also useful for the determination of food quality. A metabolomics-based study were able to predict the quality ranking on a set of green tea leaves (Pongsuwan et al. 2007). Clear discrimination between the best and the

worst ranked samples was revealed by analyzing the metabolome data using PCA. In addition, metabolic profiling found various compounds that may contribute to the quality of tea, such as sucrose, fructose, and theanine.

Metabolomic study is also widely applied for fermented products. Metabolite profiling of Japanese soy sauce was conducted to investigate the correlation between components and sensory attributes of the soy sauce (Yamamoto et al. 2012). A following study also revealed the influence of yeast and lactic acid bacterium present during the fermentation process (Harada et al. 2017). Another study about soy sauce-like seasoning investigated the effect of raw materials used for production (Yamana et al. 2020). All studies utilized GC-MS for untargeted profiling and PCA for the discrimination of the samples.

## **1.4 Mass spectrometry imaging**

### **1.4.1 General concept**

Mass spectrometry imaging (MSI) is a technique to visualize the spatial distribution of analytes on a sample cross-section based on its mass-to-charge ratio ( $m/z$ ) value. In principle, this technology does not require labeling, is able to monitor multiple analytes simultaneously, semi-quantitative, and relatively fast (Canela et al. 2016). Because of these advantages, MSI proves to be a very attractive method to visualize analytes on many kinds of samples, including human and animal tissues, plants, and even food materials (McDonnell et al. 2010; Bjarnholt et al. 2014; Handberg et al. 2015).

The basic principle of MSI is the collection of a series of mass spectra from rastering a specified area of a tissue sample (Dong et al. 2016). From each acquisition point, a whole mass spectrum is generated. The data matrix will consist of the ion, its intensity, and its x-y coordinate on the sample. From this data, it is possible to visualize the ion intensity distribution and correlate it with the sample's form and structure.

Several ion sources are available for MSI analysis. The most popular ones include matrix-assisted laser desorption/ionization (MALDI), desorption electrospray ionization (DESI), and secondary ion mass spectrometry (SIMS); each of them with its own strength and weaknesses. As such, the selection of technique depends on the objective of the study (Vickerman 2011).

#### 1.4.2 Matrix-assisted laser desorption/ionization mass spectrometry imaging

Matrix-assisted laser desorption/ionization mass spectrometry imaging (MALDI-MSI) is one of the most widely used technique for MSI. The technique is commonly applied for a wide range of samples, and high-resolution imaging (compared to DESI) is possible by modifying the laser diameter and matrix application. Figure 1.5 shows the workflow of imaging by MALDI-MSI.

- Sample sectioning

Sample sectioning is one of the most important steps in MSI analysis. Sample sectioning is usually done by cryosectioning, as the below-freezing temperature maintains the morphology of most samples during sectioning. For small samples with diameters less than 1 cm, it is common to first embed it into an embedding material before the sectioning step. The thickness of the sections used for MSI analysis ranges from 8  $\mu\text{m}$  to 100  $\mu\text{m}$ . Thinner sections are usually preferred since it is known to increase ion detectability (Sugiura et al. 2006). However, acquiring thin sections depends on the sample's sturdiness.

The sections are then mounted onto a conductive glass slide coated with Indium Tin Oxide (ITO) by thawing (Dong et al. 2016). For samples that are brittle or fragile, an adhesive film is usually used during sectioning. The film with the attached section is then mounted to a glass slide using a conductive double-sided tape (Fujino et al. 2016). The use of conductive material is especially important for MALDI instruments that employ atmospheric pressure, as it relies on electric field strength difference between sample and MS inlet to transport the ions.

- Matrix application

The sectioned sample is applied by matrix before laser irradiation. The function of the matrix is to assist desorption/ionization of target compounds as well as reducing fragmentation that may occur from high laser energy. As such, compounds that are usually used for matrix has aromatic rings in their structure, which are known to be able to absorb energy from UV lights (Leopold et al. 2018). Many matrix substances are available commercially, and each matrix has different efficiency in different analysis modes and for different groups of metabolites.

The goal of matrix application in MALDI-MSI is to evenly coat the matrix on the sample surface, as to reduce the possibility of concentrated spots that may produce higher ion intensity and hinder correct interpretation of the ion distribution. This is usually achieved by spraying dissolved matrix in a solvent to the surface of the sample. Spraying can be done manually by using an airbrush or an automatic sprayer. Another method is by sublimating the matrix powder onto the sample surface (Hankin et al. 2007). This method usually needs a special instrument to control the temperature and pressure condition of the sublimation vessel. Matrix application by spraying is generally used since it produces higher ion intensity due to the presence of solvent that could extract target compounds (Dong et al. 2016).

- MALDI-MSI analysis

Samples applied with matrix are then analyzed using a MALDI-MS instrument that is already modified to suit MSI analysis. This modification includes the software used or the ability to take pictures of the sample within the instrument. It is necessary to be able to determine the area of analysis that correlates with the sample's shape or area of interest. The laser will irradiate the samples on predetermined points with a fixed distance between each point. The samples irradiated will produce a plume of ions, which will be transported to the mass spectrometer.

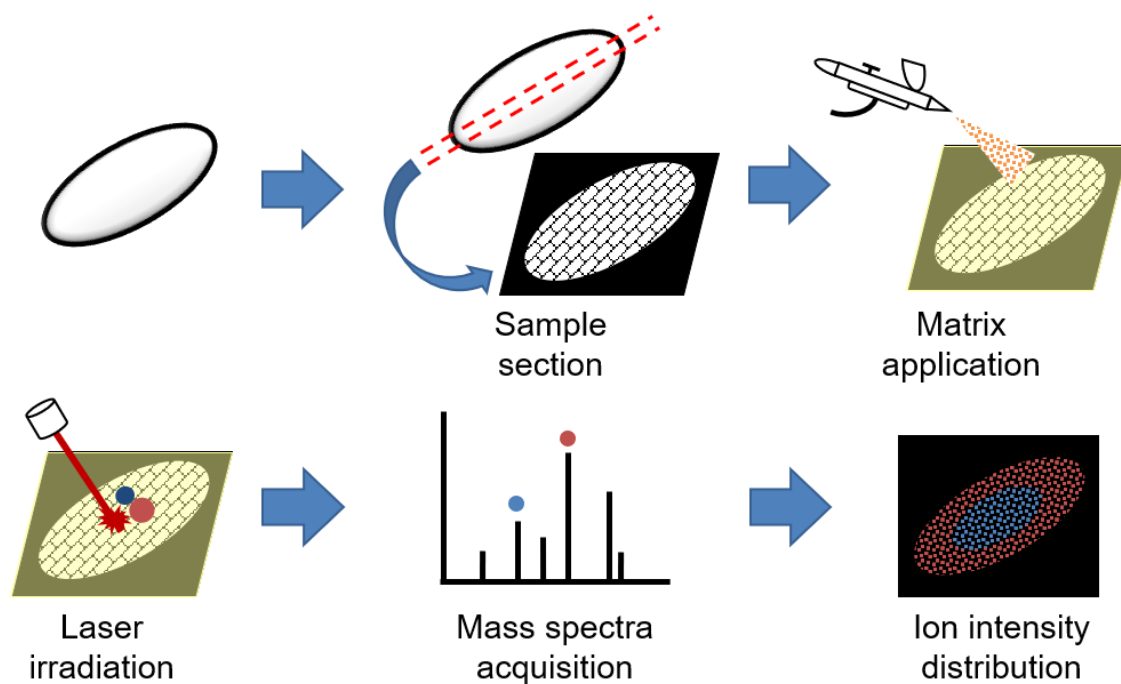


**Figure 1.5 MALDI-MSI workflow. Red and blue colored dots represent the generated ions and its distribution.**

### 1.4.3 Application of MALDI-MSI for food samples

The first application of MALDI for MSI was reported for the imaging of peptides and proteins in animal and human tissues (Caprioli et al. 1997). Many applications on different types of samples have been conducted since then, including food-related samples. The use of MSI for food analysis was employed for various applications, such as safety evaluation, characterization, authenticity investigation, quality evaluation, and toxicity check (Canela et al. 2016). The target compounds are usually lipids, peptides, and secondary metabolites such as anthocyanins or flavonoids.

Application of MSI on samples such as fruits and grains were proven to be successful in imaging numerous targeted compounds (Handberg et al. 2015). The applicability of MALDI-MSI, in particular, was already demonstrated in various researches. The spatial variability of cell-wall saccharides in wheat grain was revealed by imaging of digested polysaccharides (Veličković et al. 2014). In another study, the distribution of lysophosphatidylcholine was observed in rice grains (Zaima et al. 2014).

On the other hand, not much research aims to profile a large group of compounds. Instead, they focus on one compound that is already known to exist inside the food sample. This trend stems from the inability of current MSI systems to easily and reliably annotate the detected peaks, as it only relies on  $m/z$  information. As such, gathering initial information on the compounds inside a sample is crucial prior to MSI analysis in order to more confidently predict the detected peaks.

### **1.5 Objective of this study**

As previously stated, *haze-komi* is thought to have a high correlation with the components inside rice *koji*. However, no studies have been done based on exhaustive observation of the levels of the metabolites. Hence, metabolite level studies related to *haze-komi* is a topic of interest in the brewing industry. To facilitate the required study, it is necessary to improve the conventional visualization of the *haze-komi* profile. In addition, a correlation study between the *haze-komi* profile and the component profile inside rice *koji* would be expected.

As such, the objective of this study is to observe the trend of *haze-komi* and metabolites alteration during rice *koji*-making. Time-course analysis of rice *koji* using the combination of metabolomics and imaging techniques was planned to achieve this objective. The strategies are as follows:

- GUS reporter system histochemical assay was used for *haze-komi* visualization on a thin section of rice *koji*
- Metabolome analysis using GC- and LC-MS was applied to obtain information on component alterations during the rice *koji*-making process
- Finally, MSI was utilized for the visualization of metabolites distribution found through metabolome analysis and compared with the profile of *haze-komi*

### **1.6 Thesis outline**

This thesis includes five chapters that describe the steps in the study of *haze-komi* and metabolites distribution in rice *koji* through the combination of metabolomics and visualization approach. The first chapter provides a general introduction regarding rice *koji* and *haze-komi* as one of its prominent features, as well as scientific techniques such as GUS histochemistry, metabolomic profiling, and MSI that are promising tools for the study of *haze-komi* in rice *koji*. In chapter two, GUS histochemistry for a thin section of

rice *koji* was considered and applied for different time points during rice *koji*-making. In chapter three, the same samples from chapter two were subjected to GC-MS and LC-MS analysis to investigate the metabolite alterations during the rice *koji*-making process. In chapter four, the metabolites detected from chapter three was visualized using MSI and compared with the GUS stained sections of rice *koji* in order to see the correlation between *haze-komi* and metabolites distribution. Finally, the conclusion obtained from this study were summarized, and future perspectives were proposed in chapter five.

## Chapter 2

### Mapping of *haze-komi* using GUS staining

#### 2.1 Introduction

The quality of *koji* is finally determined by its enzyme activity and its components (Ito et al. 1989). However, in the actual production of *koji*, the quality is kept by detailed process management based on the appearance, smell, taste, hardness, and other information obtained by skilled veterans using all five senses.

Among the observations by the five senses, the visual observation of the appearance of the *koji* is especially important. Specifically, attention is paid to the presence of white spots called *haze*, which indicate the presence of mycelium, on the surface of steamed rice. The degree of mycelial penetration into the rice is called *haze-komi*, with three prominent features describing the condition of *koji* mold growth: *nuri-haze*, *tsuki-haze*, and *sou-haze*. *Nuri-haze* is defined as a condition where the *haze* covers the surface of rice grains but has only grown shallowly inwards. *Tsuki-haze* is the condition where the *haze* is seen as spots on the surface of the grain and has penetrated deep into the rice grain, while *sou-haze* is the *haze* that not only covers the whole surface of the rice grain but also has grown deep inwards. According to the National Research Institute of Brewing (NRIB), *tsuki-haze* and *sou-haze* are considered to result in good rice *koji* and have different effects on the taste of *sake*.

The observation of *haze-komi* on rice *koji* has garnered attention for a long time. Some researchers have described the effort on whole rice *haze-komi* observation through transmitted light microscope (Ito et al. 1989) or camera image analysis (Ito et al. 2016). While these methods are fairly simple, they employ empirical approach based on the white areas of *haze*, which may not reflect accurate mycelial distribution. To specifically detect *haze-komi*, the reporter system using  $\beta$ -glucuronidase (GUS) is a promising technique as it has low or non-detectable activity in higher plants and fungi. The use of the system to perform histochemical staining was first demonstrated by adding glucuronide substances to a transformed tobacco plant (Jefferson et al. 1987). Applicability of the GUS system for filamentous fungi was then proven when *Aspergillus nidulans* and *Aspergillus flavus* (Roberts et al. 1989), as well as *A. oryzae* (Tada et al. 1991), were successfully transformed and used to study gene expression. Some studies

also reported the use of this system to detect fungal infection in plant tissues (Oliver et al. 1993; Brown et al. 1997), demonstrating its usefulness to observe fungal mycelia growth in a media.

In this chapter, the GUS histochemical staining was adapted to visualize *haze-komi* during rice *koji*-making. A GUS-expressing *A. oryzae* strain was constructed and used to produce rice *koji*. Time-course sampling was then conducted to observe the progression of *haze-komi* during the course of rice *koji* production.

## 2.2 Experimental

### 2.2.1 *Aspergillus oryzae* GUS strain construction

The *A. oryzae* GUS strain was constructed as described in a previous study (Tsuboi et al. 2005). The recipient strain was *A. oryzae* *niaD*300 strain (*niaD*<sup>-</sup>). The plasmid vector pGEM-T easy (Promega Corporation, Madison, WI, USA) was modified to harbor the *A. oryzae* P-*enoA*, *Escherichia coli uidA*, and *A. oryzae niaD*, as a promoter, reporter, and selectable marker gene, respectively. The plasmids were then introduced into *A. oryzae* by *niaD*-based homologous recombination, while transformation was carried out according to a previously described method (Gomi et al. 1987). (*Strain construction was conducted in Tohoku University by collaborator, Prof. Katsuya Gomi*)

### 2.2.2 Rice *koji* making

*A. oryzae* GUS strain was cultured in potato dextrose (PD) agar plate at 30°C for 5 days. Conidia suspension was recovered from the culture and was diluted with Tween 80 to achieve number of conidia  $3.0 \times 10^7$  per mL. A total of 30 g *Hakutsuru Nishiki*-type polished rice (polishing ratio, 70%; water content, 12.4%) was used as the culture substrate. The steamed rice (water absorption 29%) was inoculated with the conidia inside a polypropylene container (conidia intake approximately  $3.0 \times 10^5$  per gram rice) and placed in a thermostatic chamber – SH-221 (Tabai Espec, Osaka, Japan). The *koji* mold was cultured for 43 h with growth conditions as described in Table 2.1, stirring occasionally performed at 24- and 31-hour mark. Sampling was done at the 24-, 31- and 43-hour mark. The RIB40 strain as a negative control was also prepared with the same procedure. (*Rice koji making were done in Hakutsuru Sake Brewing company by collaborator, Yoshihiro Tamada*)

**Table 2.1 Temperature and humidity condition in rice *koji*-making**

<b>Time (h)</b>	<b>Temperature (°C)</b>	<b>Humidity (%)</b>
0 – 19	32	95
19 – 31	35	90
31 - 43	38	85

### **2.2.3 Mycelia content estimation**

The mycelia content estimation procedure was based on a previous report (Fujii et al. 1992). Rice *koji* was dry heated at 100°C for 1 hour and milled for 3 minutes in Hi-speed Vibration Sample Mill TI-100 (CMT, Tokyo, Japan). The milled rice *koji* was then washed with 50 mM phosphate buffer pH 7.0 and centrifuged for 10 minutes at 3000 rpm, followed by removing the supernatant. The washing procedure was repeated three times. Yatalase enzyme T017 (Takara, Shiga, Japan) was added along with phosphate buffer and mixed thoroughly before incubated in a shaker at 37°C for 1 hour with 180 rpm speed. After centrifugation for 10 minutes at 3000 rpm, the supernatant was passed through a 0.45 µm cellulose acetate membrane filter (Advantec, Tokyo, Japan). The filtrate was then diluted with distilled water and used as the sample for mycelia content estimation. A calibration curve of N-acetylglucosamine (GlcNAc) content was first constructed by preparing standard solutions of 0, 25, 50, and 100 µg/mL. The sample was added with 0.8 M potassium tetraborate and boiled for 5 minutes. A p-dimethylaminobenzaldehyde (p-DMAB) solution was prepared by dissolving the powder in acetic acid containing 12.5% 10 N HCl and diluted 10-fold before added to the cooled down sample and left at 37°C for 20 minutes. The solution was then analyzed using Microplate Reader Infinite M200 (Tecan, Männedorf, Switzerland) to read the absorbance at 585 nm. All samples were analyzed in triplicate. The GlcNAc concentration of each sample was calculated from the standard calibration curve. The number of cells was calculated on the assumption that 1 mg of cells contained 139 µg of GluNAc. (*Mycelia content estimation were done in Hakutsuru Sake Brewing company by collaborator, Yoshihiro Tamada*)

### **2.2.4 Rice *koji* sectioning**

One grain of rice *koji* sample was first embedded in a mold (Base mold A, Falma, Tokyo, Japan) using 4% carboxymethylcellulose (CMC) (Leica Microsystems, Wetzlar,

Germany) and frozen at  $-80^{\circ}\text{C}$ . The frozen sample block was attached to the sample holder using the optimal cutting temperature compound (OCT) (Surgipath FSC 22, Leica Biosystems, Nussloch, Germany) before sectioning inside a cryostat (CM1950, Leica Biosystems, Nussloch, Germany). From the approximate center of the rice *koji* grain, longitudinal sections with  $20\ \mu\text{m}$  thickness were obtained. Adhesive cryofilm (type II C(10), SECTION-LAB, Hiroshima, Japan) was used to acquire the sample sections. Chamber temperature and sample holder temperatures were  $-20^{\circ}\text{C}$  and  $-16^{\circ}\text{C}$ , respectively. The films with the section were taped on a glass slide (Matsunami Glass, Osaka, Japan) for histochemical staining.

### **2.2.5 Histochemical staining and observation**

A stock solution of histochemical staining substrate was first prepared by dissolving X-Gluc powder (TCI Chemicals, Tokyo, Japan) in methanol. A spraying solution of 5 mM X-Gluc in phosphate buffer pH 7.0 containing 0.1 M  $\text{NaH}_2\text{PO}_4$  and 0.1 M  $\text{Na}_2\text{HPO}_4$  (1:1, v/v) was then prepared using the stock solution. The substrate was applied to the sample section by spraying using an airbrush spray (Procon BOY FWA Double Action Platinum 0.2, GSI Creos, Tokyo, Japan) at room temperature. The sample was then stored in a sealed tube containing phosphate buffer-soaked tissue to maintain humidity and was placed in an incubator at  $37^{\circ}\text{C}$  for 2 h. The sample was then transferred to a container with silica gel to absorb the water content before observation. *Koji* mold growth in the rice *koji* was examined by observing the indigo color using a stereomicroscope (SZX7, Olympus, Tokyo, Japan) equipped with a digital camera (OLYMPUS PEN EPL9, Olympus, Tokyo, Japan).

## **2.3 Results and discussion**

### **2.3.1 Rice *koji* sectioning**

A good morphology section is important in order to clearly observe the mycelial distribution in rice *koji*. In common practice, frozen tissue sections are usually acquired by using brush to hold the section as the blade runs through the sample block. With this, large and firm tissues such as animal tissue can be easily cut. On the other hand, rice *koji* is small and fragile, making it very difficult to make a section. As such, optimization of sectioning method is required for rice *koji*.

Aiding tools such as anti-roll plate and adhesive cryofilm were used to help obtain a rice *koji* section with good morphology. Anti-roll plate is a glass plate that holds sample section as it was cut so that the section will not curl. Another method using adhesive cryofilm (Kawamoto 2003) includes taping the film to the cross-section of sample, so that the acquired section will stick to the film. The two methods were compared with the conventional method, as can be seen in Figure 2.1. The rice *koji* made by *A. oryzae* RIB40 strain was used to evaluate the methods. The conventional and anti-roll plate method resulted in rice *koji* sections with holes. On the other hand, cryofilm was able to keep the form of rice *koji*, acquiring a good morphology section. The sectioning method using cryofilm was then applied to acquire section for histochemical staining.

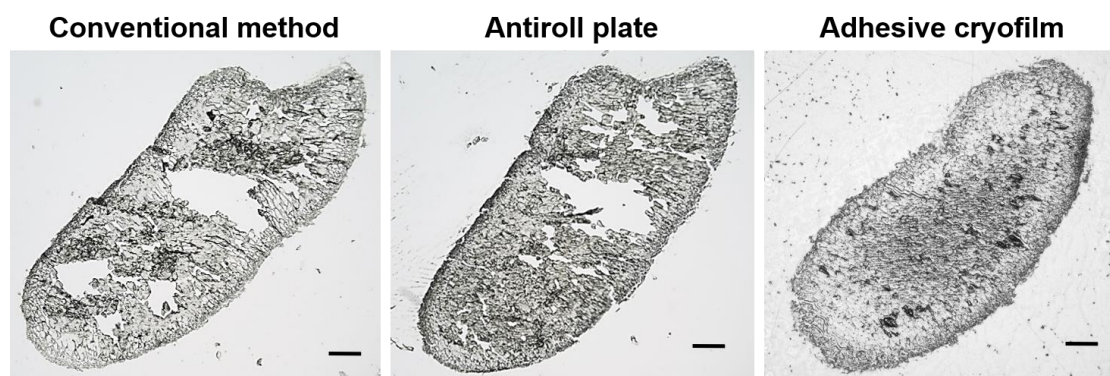


**Figure 2.1 Rice *koji* sectioned with different methods. Scale bar is 500  $\mu$ m**

### **2.3.2 Time-course observation of *haze-komi* in rice *koji***

The surface of rice *koji* from each time point was observed for the existence of *haze*. The surface photo is shown in Figure 2.2. The surface of steamed rice was not completely covered by *haze* at 24 hours after inoculation. At 31- and 43-hour time point, mycelia extension on the surface are more pronounced. However, surface *haze* could not fully demonstrate the state of mycelia penetration into the steamed rice. Thus, rice *koji* inoculated with the *A. oryzae* GUS strain was utilized to observe *haze-komi* during the *koji* making process.



**Figure 2.2 Surface photo of rice *koji* at 24-, 31-, and 43-hour time point. Scale bar is 1 mm**

The common method of GUS staining involves incubating the sample inside the X-Gluc buffer solution for a certain period of time. However, this method is only possible for samples that do not change their form upon contact with liquid. Samples such as steamed rice and rice *koji* easily absorb water, leading to the deformation of their shape when submerged for a prolonged period. On the other hand, the X-Gluc substrate will not be able to permeate through the cell walls and react without sufficient time. This prompted another approach by spraying the X-Gluc substrate on the cross-section of rice *koji*. Several adjustments were made in order to obtain an indigo color distribution that would best represent the *A. oryzae* mycelia penetration, such as the concentration of X-Gluc substrate to be applied as well as the incubation method. The new method was tested on rice *koji* made with GUS-expressing *A. oryzae*. Un-inoculated steamed rice, as well as rice *koji* made using a normal strain of *A. oryzae* RIB40, were also used as controls. The result can be seen in Figure 2.3. Indigo color was seen clearly on the cross-section of rice *koji* made with GUS-expressing *A. oryzae*. No indigo color was observed on both the control samples after X-Gluc substrate spraying and incubation, confirming that there was no or negligible GUS activity in rice and *A. oryzae* itself.

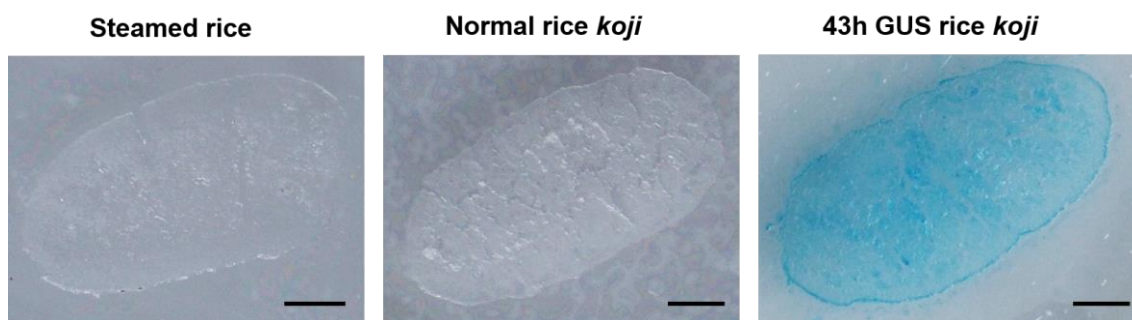


**Figure 2.3 GUS-stained steamed rice, normal rice *koji*, and 43-hour time point rice *koji*. Scale bar is 1 mm**

The developed method was then applied to the rice *koji* of all sampling points, as seen in Figure 2.4. After fungal inoculation for 24 hours, GUS was observed to be expressed in certain areas on the surface of the steamed rice grain (Figure 2.3A). With higher magnification, it was revealed that the indigo color was also observed under the surface of grain (Figure 2.3B). This result indicated that 24 hours after inoculation, the hyphae of *A. oryzae* had already penetrated shallowly into the steamed rice. Moreover, the indigo color was perceived to be more intense on the edges of endosperm cells, suggesting that the fungal hyphae penetrated between the rice endosperm cells. The process of rice *koji* making is a type of solid-state fermentation. In this condition, filamentous fungi are confronted by nutrient gradients (Te Biesebeke et al. 2002). The source of carbon needed for growth is present inside the substrate, while oxygen is mainly available at the surface. This condition may have driven the fungi to first concentrate their growth into the substrate and collect the carbon for further growth on the surface.

At 31 hours after inoculation, complete color alteration as well as an increase in color density on the surface of rice *koji* can be observed (Figure 2.3C). Compared to the condition at 24-hour time point, the indigo color had spread further on the whole surface of the rice *koji* section, showing the condition of *sou-haze*. This indicated that the fungal mycelia have completely penetrated and covered the entire grain. By the 43-hour time point, an even deeper indigo color was observed on the section, especially on the surface of rice *koji* (Figure 2.3E&F).

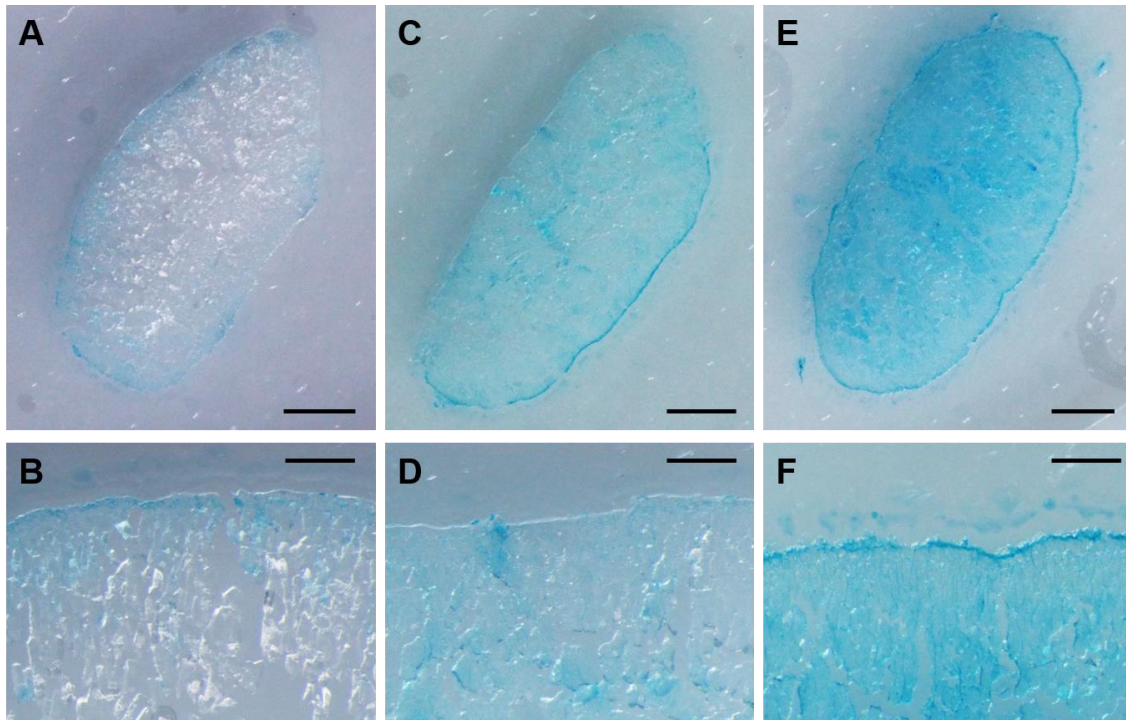


**Figure 2.4 Stained GUS rice *koji* at (A, B) 24-, (C, D) 31-, and (E, F) 43-hour time point. Scale bar for A, C, and E is 1 mm. Scale bar for B, D, and F is 200  $\mu$ m.**

The color intensity trend suggested that *A. oryzae* propagate further on the surface of steamed rice at a much later phase of rice *koji* making. It is known that filamentous fungi gain competence to form aerial hyphae faster when the colony becomes older (Krijgsheld et al. 2013). This tendency may explain the stronger indigo color on the surface of steamed rice after longer fermentation. The color may also imply the branching of hyphae mainly around the surface of steamed rice. Furthermore, the fungi had spread almost completely inside the steamed rice within several hours after one day of inoculation. This may indicate that *A. oryzae* grew exponentially on rice between the 24-hour to 31-hour mark. A similar observation was reported based on fluorescent-labeled antibody visualization (Kojima et al. 1999). However, their report did not show a complete mycelia coverage in rice *koji* after 31 hours. This may be due to different properties of samples as well as the rice *koji*-making process used in the study.

As the staining method in this study relies on the GUS enzyme, the secretion profile of said enzyme is of valid concern. A study has demonstrated the localization of the GUS staining product inside the mycelium of a transformed *A. niger* (Gottschalk et al. 1996), which implied that the enzyme is expressed intracellular. While there are no reports on

the GUS secretion profile of transformed *A. oryzae* in a solid-media, the color distribution difference between 24-hour time point and 31- or 43-hour time point suggested that GUS was intracellular or at the least not diffused too far from the fungal mycelia. As such, the GUS system should be accurate enough to indicate the changes of mycelia distribution in this study.

## **2.4 Conclusion**

In this study, an alternative method for the observation of *haze-komi* was presented by the use of the GUS reporter assay. The progression of *haze-komi* during rice *koji*-making process was successfully visualized using GUS staining. The staining approach provides a clear mapping of mycelial distribution on a thin rice *koji* section, both for the whole section or higher magnification observation.

## Chapter 3

### Time-course metabolite profiling of rice *koji*

#### 3.1 Introduction

One of the roles of the rice *koji* is to provide various metabolites that may contribute to the process of main fermentation or even affect the characteristic of end products. As such, many researchers have pursued the profiling of rice *koji* metabolites. These studies focused on the effects of materials involved, such as the fungal strain used (Kim et al. 2010; Lee et al. 2016) or the polishing rate of rice (Lee et al. 2018). Some reported the changes during a time-course observation, in which different classes of metabolites such as sugars, amino acids, and organic acids fluctuated during the process. Nevertheless, the discussions are more focused on the effects of materials rather than the time-related changes.

Additionally, comprehensive metabolite profiling of rice *koji* with more consideration on amino acids and other amine metabolites profiles is still missing. Rice *koji* is known to produce various amino acids (Ito et al. 2013), and further exploration would be expected. Furthermore, the production of polyamines by rice *koji* has been a topic of interest due to its nutritional benefits. An exhaustive metabolite profiling including amino acids and polyamines would be beneficial.

In this chapter, rice *koji* was subjected to untargeted metabolite profiling using GC-MS as well as amino acids and other amines profiling by LC-MS in order to obtain comprehensive information on the metabolite changes during rice *koji* production.

#### 3.2 Experimental

##### 3.2.1 Samples and chemicals

*Hakutsuru nishiki*-type (polishing rate 70%) steamed rice and rice *koji* made with GUS-expressing *A. oryzae* were obtained as described in the experimental section of chapter 2. The rice *koji* was sampled at 24-, 31- and 43-hour time points. Internal standards ribitol and DL-alanine-d4 were purchased from Fujifilm Wako Pure Chemical Corporation (Osaka, Japan) and Santa Cruz Biotechnology (Dallas, TX, US), respectively. For the preparation of solvents and mobile phase, methanol (MeOH) and acetonitrile (ACN) were purchased from Kanto Chemical Co., Inc. (Tokyo, Japan). Ethanol (EtOH), pyridine, and trifluoroacetic acid (TFA) were obtained from Wako. Chloroform (CHCl<sub>3</sub>)

was purchased from Kishida Chemical Co. Ltd. (Osaka, Japan). Ultrapure water was obtained through Barnstead GenPure xCAD Plus water purification system by Thermo Fisher Scientific (Tokyo, Japan). For the derivatization process before GC-MS analysis, methoxyamine hydrochloride was purchased from Merck & Co. Inc. (Rockville, MD, US), while N-methyl-N-trimethylsilyl-trifluoroacetamide (MSTFA) were obtained from GL Sciences Inc. (Tokyo, Japan).

### **3.2.2 Sample extraction for GC-MS and LC-MS analysis**

Steamed rice and rice *koji* from all time points were frozen, milled to a fine powder, and lyophilized to remove water content. Samples were then kept at  $-30^{\circ}\text{C}$  until extraction before each analysis. Three replicates of each sample were weighed to 30 mg and added with 1 mL of a mixed solvent consisting of MeOH, ultrapure water, and  $\text{CHCl}_3$  (5/2/2, v/v/v); containing internal standard (ribitol 0.06 mg/mL for GC analysis, 0.4 mg/mL DL-alanine-d4 for LC analysis). The samples were then vortex incubated for 30 min ( $37^{\circ}\text{C}$ , 1200 rpm). After centrifugation for 3 min ( $4^{\circ}\text{C}$ , 10000 rpm), 600  $\mu\text{L}$  of the supernatant was transferred to a new microtube, added with 300  $\mu\text{L}$  ultrapure water and vortexed. Centrifugation was carried out afterward to separate the hydrophilic and hydrophobic fractions. The hydrophilic phase was used further for analysis using both GC-MS and LC-MS.

### **3.2.3 Derivatization for GC-MS analysis**

From extracted samples, 200  $\mu\text{L}$  of the upper hydrophilic phase from all samples were pooled as quality control (QC) samples, while another 200  $\mu\text{L}$  were transferred to new microtubes. All samples were then evaporated using a centrifuge concentrator at room temperature ( $25^{\circ}\text{C}$ ), followed by overnight lyophilization. Oximation was done by adding 100  $\mu\text{L}$  of methoxyamine hydrochloride dissolved in pyridine (20 mg/mL) to lyophilized samples and vortex incubated for 90 min ( $30^{\circ}\text{C}$ , 1200 rpm). The second step of derivatization by silylation was then conducted by adding 50  $\mu\text{L}$  of MSTFA to the samples and vortex incubated for 90 min ( $37^{\circ}\text{C}$ , 1200 rpm). The derivatized samples were subjected to 3 min centrifugation at room temperature before transferring them to vials for GC-MS analysis.

### 3.2.4 GC-MS analysis

A GC coupled with quadrupole MS was used for this study (GC-MS QP2010 Ultra; Shimadzu, Kyoto, Japan). The instrument was equipped with Inert Cap 5 MS/NP column; 0.25 mm × 30 m, 0.25 μm, (Varian Inc., Palo Alto, CA, USA) and autosampler AOC-20i/s (Shimadzu, Kyoto, Japan). One microliter of the derivatized sample was injected in split mode, 25:1 (v/v). The injection temperature was 270°C. The gas flow of the carrier gas He was 1.12 mL/min with a 39 cm/s linear velocity. Column temperature was controlled during analysis. Starting temperature was at 80°C, held for 2 minutes. The temperature was then increased gradually by 15°C/min to 330°C for 16 minutes, and held for 6 minutes. The transfer line temperature was 250°C, while the ion source temperature was 200°C. Electron ionization (EI) generated the ions at 0.93 kV. Mass spectra were recorded at 10000 u/s over the mass range  $m/z$  85 – 500. Standard alkane mixture (C8-C40) was also injected before the samples as a reference for retention time data and tentative identification.

### 3.2.5 LC-MS analysis

LC-MS analysis was conducted based on the previously reported method for amino acid analysis (Nakano et al. 2019) with several modifications. LCMS-8060 (Shimadzu, Kyoto, Japan) was operated in positive mode with MRM analysis mode for the detection of amino acids, polyamines, and other amines. The mobile phase consisted of a mixture of ACN, EtOH, ultrapure water, and TFA (80/15/5/0.5, v/v/v/v). From extracted samples, 50 μL were diluted with 150 μL of the mobile phase and centrifuged for 10 min (4°C, 10000 rpm). Approximately 100 μL of the diluted samples were then transferred to vials for LC-MS analysis. Chromatographic separation was achieved with CROWNPAK CR-I (+) (3.0 mm i.d. × 150 mm, 5 μm) (Daicel CPI, Osaka, Japan) as the analytical column. The flow rate of mobile phase was set at 0.4 mL/min in isocratic condition.

### 3.2.6 Data processing and multivariate analysis

The raw chromatographic data from GC-MS analysis were converted into ANDI (Analytical Data Interchange Protocol) files using GC-MS Solution software package (Shimadzu, Kyoto, Japan). Peak alignment and annotation of the converted GC-MS data were processed using MS-DIAL (Tsugawa et al. 2015) (RIKEN, Yokohama, Japan). The peak intensity of each annotated metabolites was then normalized against that of ribitol

internal standard. The peak area corresponding to each metabolite was then integrated into Excel sheets. LC-MS data analysis was performed using LabSolutions (Shimadzu). The peak area corresponding to each metabolite was then integrated into Excel sheets, followed by normalization to the internal standard, DL-alanine-d4. The resulting data matrix from both GC-MS and LC-MS analyses was then used for principal component analysis (PCA) using commercial software, SIMCA-P+ (Umetrics, Umeå, Sweden).

### **3.3 Results and discussion**

#### **3.3.1 Time-course metabolite profiling of rice *koji***

Steamed rice and rice *koji* samples were subjected to GC-MS analysis for metabolic profiling, resulting in a total of 62 metabolites tentatively annotated from all samples based on the in-house library. Sugars, sugar alcohols, amino acids, and organic acids were included in the annotated peaks. Additionally, LC-MS analysis was also conducted to broaden the metabolite coverage by adding targeted analysis of amino acids, polyamines, and amino acid-related metabolites. A total of 30 metabolites were able to be detected with the system. Additionally, the LC-MS method used was also able to separate between L- and D- forms of amino acids. From the result, it was revealed that all detected amino acids were L- forms of amino acids. The list of detected metabolites from GC-MS and LC-MS analysis can be found in Table 3.1 and 3.2, respectively.

**Table 3.1 List of metabolites detected from GC-MS analysis**

No	Metabolite name	No	Metabolite name
1	1,6-Anhydroglucose	32	Isoleucine
2	Arabinose	33	Leucine
3	Fructose	34	Phenylalanine
4	Gentiobiose	35	Proline
5	Glucose	36	Serine
6	Glyceraldehyde	37	Threonine
7	Lactose	38	Tryptophan
8	Maltose	39	Tyrosine
9	Maltotriose	40	Valine
10	Melibiose	41	GABA
11	Panose	42	4-Hydroxybenzoic acid
12	Raffinose	43	4-Hydroxyphenylacetic acid
13	Ribose	44	Fumaric acid
14	Sorbose	45	Gluconic acid
15	Sucrose	46	Isocitric/Citric acid
16	Trehalose	47	Lactic acid
17	Arabitol	48	Malic acid
18	Glycerol	49	Myristic acid
19	Inositol	50	Nicotinic acid
20	Lactitol	51	Pyroglutamic acid
21	Mannitol	52	2-Aminoethanol
22	Meso erythritol	53	3,4-Dihydroxybenzoate
23	Sorbitol	54	3-Hydroxy-3-methylglutarate
24	Threitol	55	Glucono-1,5-lactone
25	Xylitol	56	Hypotaurine
26	Alanine	57	Hypoxanthine
27	Asparagine	58	Ketovaline
28	Aspartic acid	59	Uracil
29	Glutamic acid	60	Urea
30	Glutamine	61	Uridine
31	Glycine	62	Putrescine

**Table 3.2 List of metabolites detected from LC-MS analysis**

No	Metabolite name	No	Metabolite name
1	L-Alanine	16	L-Phenylalanine
2	L-Arginine	17	DL-Proline
3	L-Asparagine	18	L-Serine
4	L-Aspartic acid	19	L-Threonine
5	L-Cysteine	20	L-Tryptophan
6	GABA	21	L-Tyrosine
7	L-Glutamic acid	22	L-Valine
8	L-Glutamine	23	Agmatine
9	Glycine	24	Cadaverine
10	L-Histidine	25	Putrescine
11	L-Isoleucine	26	Spermidine
12	L-Leucine	27	Spermine
13	L-Lysine	28	Betaine
14	L-Methionine	29	Hypotaurine
15	L-Ornithine	30	N,N-dimethylglycine

The GC-MS and LC-MS data sets were then used to examine the difference in the metabolome profile between the rice *koji* samples by multivariate analysis PCA, as seen in Figure 3.1. The PCA score plots showed a clear separation between each sample based on the PC1 and PC2 axis (PC1 64.4%, PC2 19.6%). Simultaneously, the loading plots reveal that most of the detected metabolites were positively correlated with rice *koji* samples. The PC1 axis especially showed separation based on the fermentation time, while the PC2 axis separates samples based on the content of tri- and di-saccharides. The relative intensity of detected metabolites was then compared between each sample.

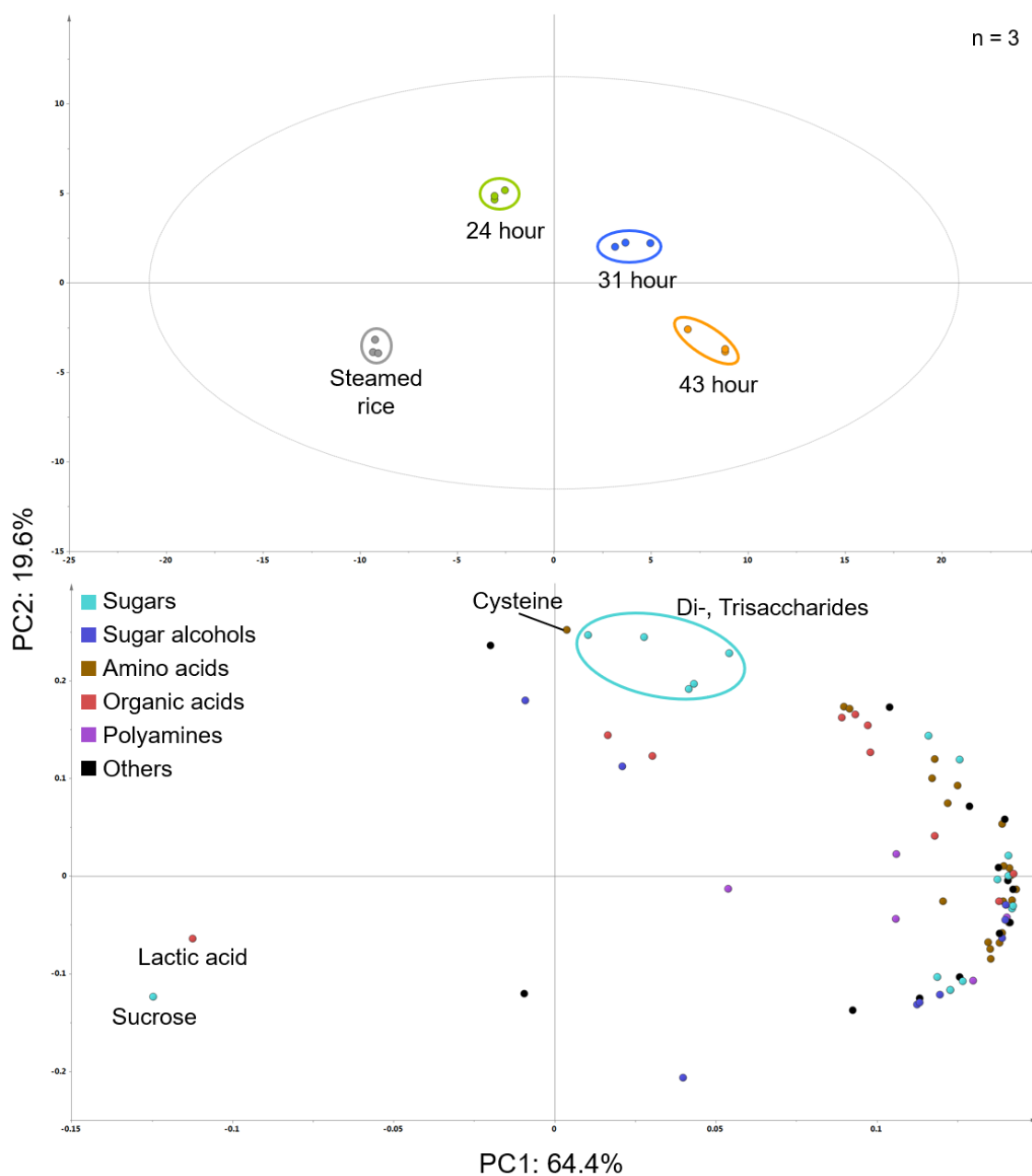


**Figure 3.1** Score plot (above) and loading plot (below) based on combined results from GC- and LC-MS analysis. Scaling method: UV, transformation: none.

### 3.3.2 Changes in sugar and sugar alcohols profile during rice *koji*-making

Alterations of all annotated sugars and sugar alcohols were observed during the rice *koji*-making process. Bar graphs of the detected sugars can be found in Figure 3.2.

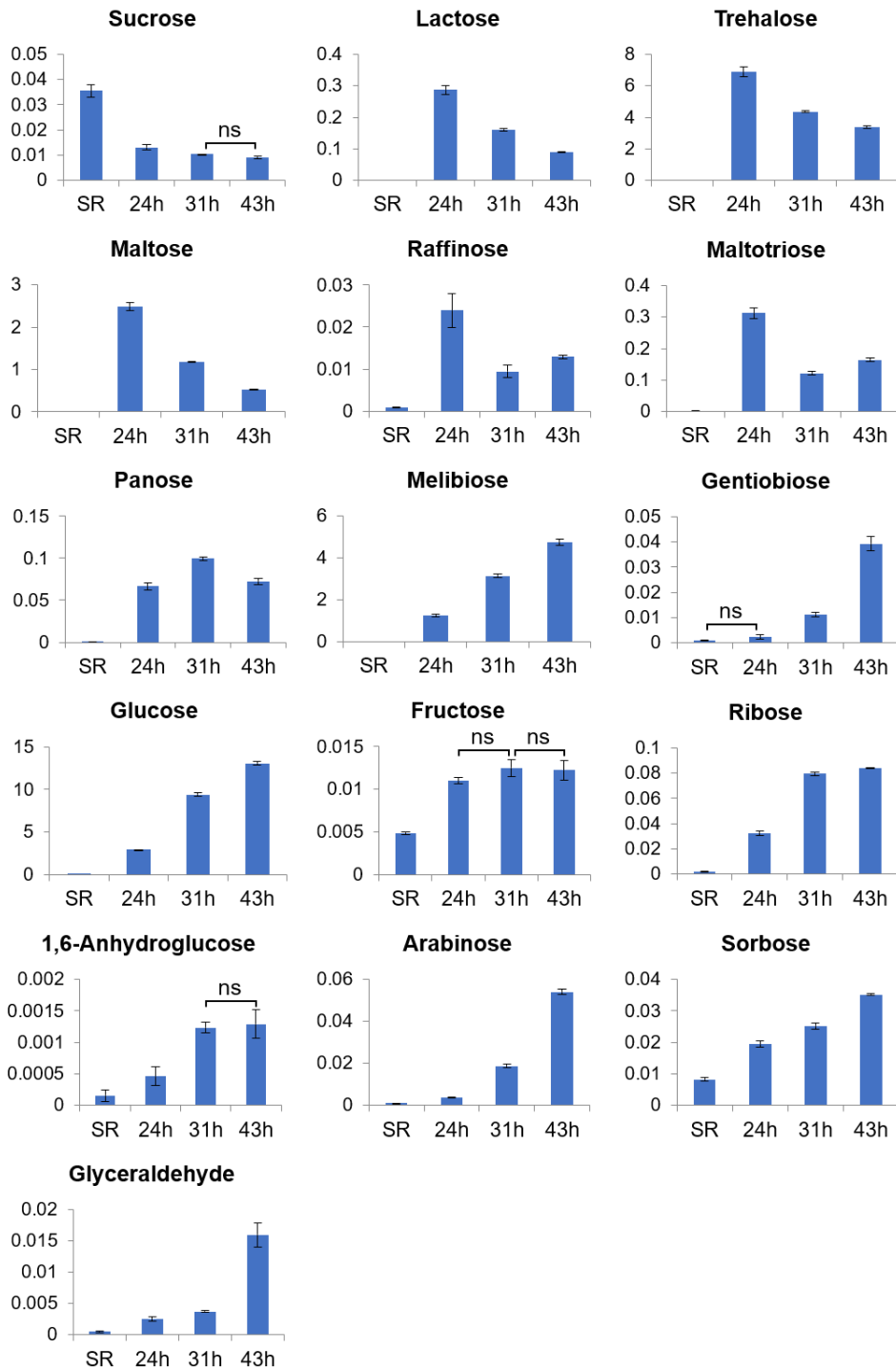


**Figure 3.2** Relative intensity of sugars during rice *koji*-making. X-axis represents sampling points (SR: steamed rice), while Y-axis represents relative intensity towards the internal standard. Changes between time points are significant ( $p < 0.05$ ), unless denoted (ns).

Sucrose, which is shown to be higher in steamed rice, significantly decreased after 24 hours into the process. Furthermore, several disaccharides such as lactose, trehalose, and maltose, as well as trisaccharides such as raffinose and maltotriose, increased during the same time before decreasing as the process continued. Other polysaccharides such as panose, gentiobiose, melibiose still exhibited an increasing trend after 24 hours, with the exception of panose decreasing after the 31-hour time point. On the other hand, an increasing trend of various monosaccharides such as glucose, fructose ribose, sorbose, arabinose, and glyceraldehyde can be observed during the rice *koji*-making process. Sugar alcohols generally showed an increasing trend with the exception of lactitol and sorbitol, as seen in Figure 3.3. The two sugar alcohols peaked at the 24-hour time point and significantly decreased at the 31-hour time point before increasing again after 43 hours of the process.

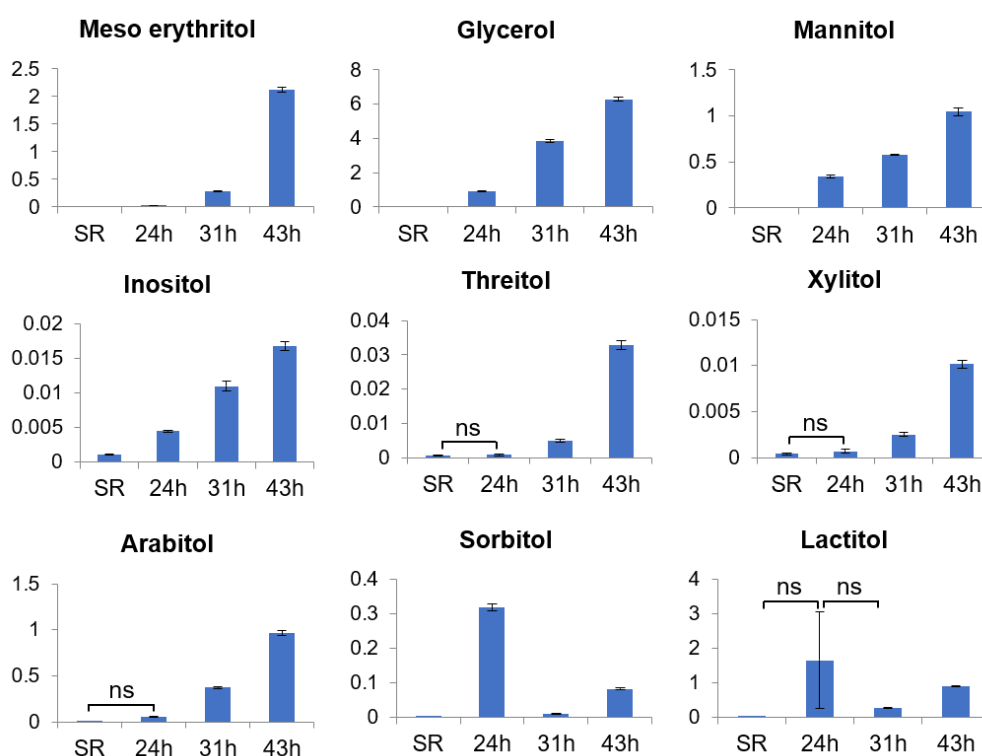


**Figure 3.3** Relative intensity of sugar alcohols during rice *koji*-making. X-axis represents sampling points (SR: steamed rice), while Y-axis represents relative intensity towards internal standard. Changes between time points are significant ( $p < 0.05$ ), unless denoted (ns).

The high amount of sugars and sugar alcohols produced during rice *koji*-making signified that amylolytic enzymes were produced by the fungi *A. oryzae* to break down the high amount of starch in steamed rice. *A. oryzae* is known to produce high amount of amylolytic enzymes such as  $\alpha$ -amylase and glucoamylase in solid-state fermentation (Oda et al. 2006). The  $\alpha$ -amylase work first by randomly cleaving the starch into glucose oligomers. The glucoamylase then gradually transformed the reduced sugars into glucose. The step-by-step process was clearly indicated by how trisaccharides and disaccharides increased first at 24-hour before decreasing gradually, leading to the production of monosaccharides. Additionally, it has been reported that filamentous fungi such as *A. oryzae* tend to accumulate sugar alcohols at low water activity ( $a_w$ ) environment (Ruijter et al. 2004). Rice *koji*-making is a type of solid-state fermentation, and as such, has a low  $a_w$  environment.

### **3.3.3 Changes in amino acids profile during rice *koji*-making**

All of the detected amino acids in this study were shown to be increased after the rice *koji*-making process, as shown in Figure 3.4. The result confirmed the findings from previous studies, where the increase of amino acids was observed after rice *koji*-making (Lee et al. 2018; Ito et al. 2013). As *A. oryzae* needs a nitrogen source for its growth, protease and carboxypeptidase were produced to breakdown the proteins inside the rice (Matsunaga et al. 2002).

Among the increased amino acids, cysteine was immediately decreased after 24 hours, implying that *A. oryzae* mainly utilized the cysteine during its growth. A previous study also mentioned that the production of cysteine during rice *koji*-making is lower than other amino acids (Ito et al. 2013). Several amino acids such as glutamic acid, glycine, methionine, serine, tryptophan, tyrosine, arginine, and asparagine did not increase significantly after 31h. On the other hand, significant decrease of valine, leucine, isoleucine, and phenylalanine after 31h was observed. The branched chain amino acids, valine, leucine, and isoleucine are involved in the production of various volatile compounds such as 3-methyl-1-butanol and 2-methyl-1-butanol through the Ehrlich pathway (Ji et al. 2017). These compounds were also detected in vapor analysis of rice *koji* (Yoshizaki et al. 2010). Phenylalanine degradation may also be related to production of phenylacetaldehyde, a flavor volatile compound detected in rice *koji*.

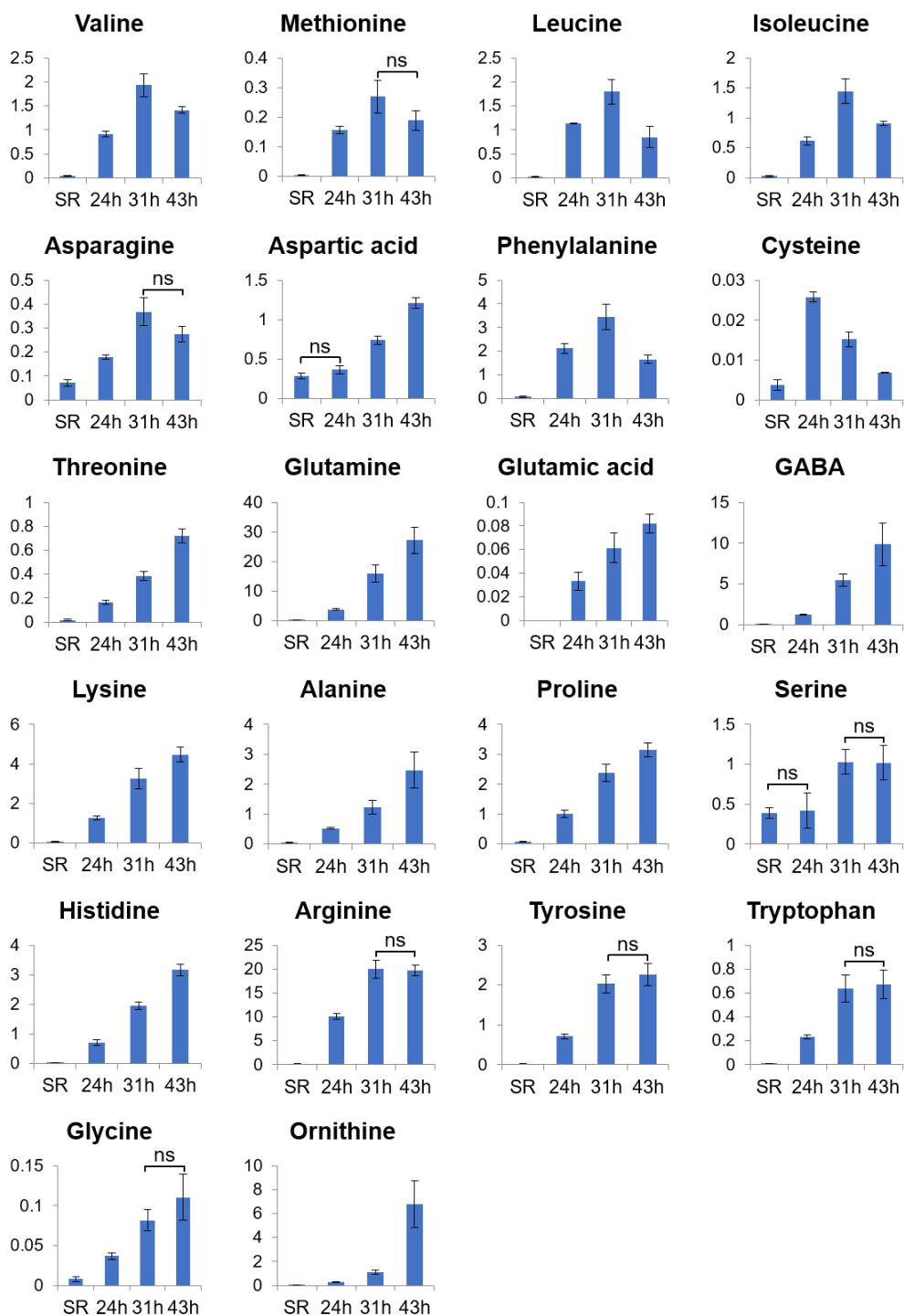


**Figure 3.4** Relative intensity of amino acids during rice *koji*-making. X-axis represents sampling points (SR: steamed rice), while Y-axis represents relative intensity towards the internal standard. Changes between time points are significant ( $p < 0.05$ ), unless denoted (ns).

### 3.3.4 Changes in other metabolites during rice *koji*-making

Most organic acids showed an increasing trend during rice *koji*-making except for lactic acid, presented in Figure 3.5. Previous study mentioned that there were no reports of functional lactate dehydrogenase in *Aspergillus* (Dave and Punekar 2015), which may explain the lack of lactic acid production in rice *koji*. Pyroglutamic acid and gluconic acid exhibited a steady increase, while other organic acids peaked at different times during the rice *koji*-making process. Dynamic changes of fumaric acid, malic acid, and citric acid may indicate the activity of the TCA cycle during *A. oryzae* growth. Myristic acid levels were mostly unperturbed during the process. The detection of myristic acid in steamed rice confirmed that the fatty acid existed in the rice (Yasumatsu and Moritaka 1964).

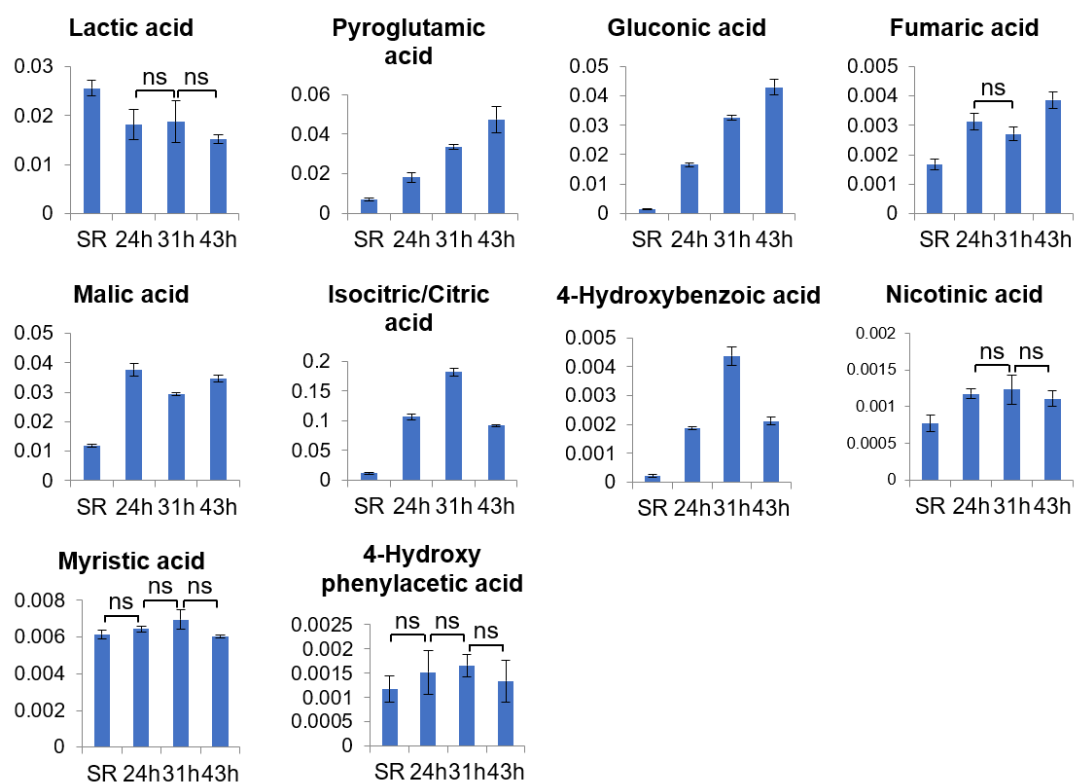


**Figure 3.5** Relative intensity of organic acids during rice *koji*-making. X-axis represents sampling points (SR: steamed rice), while Y-axis represents relative intensity towards the internal standard. Changes between time points are significant ( $p < 0.05$ ), unless denoted (ns).

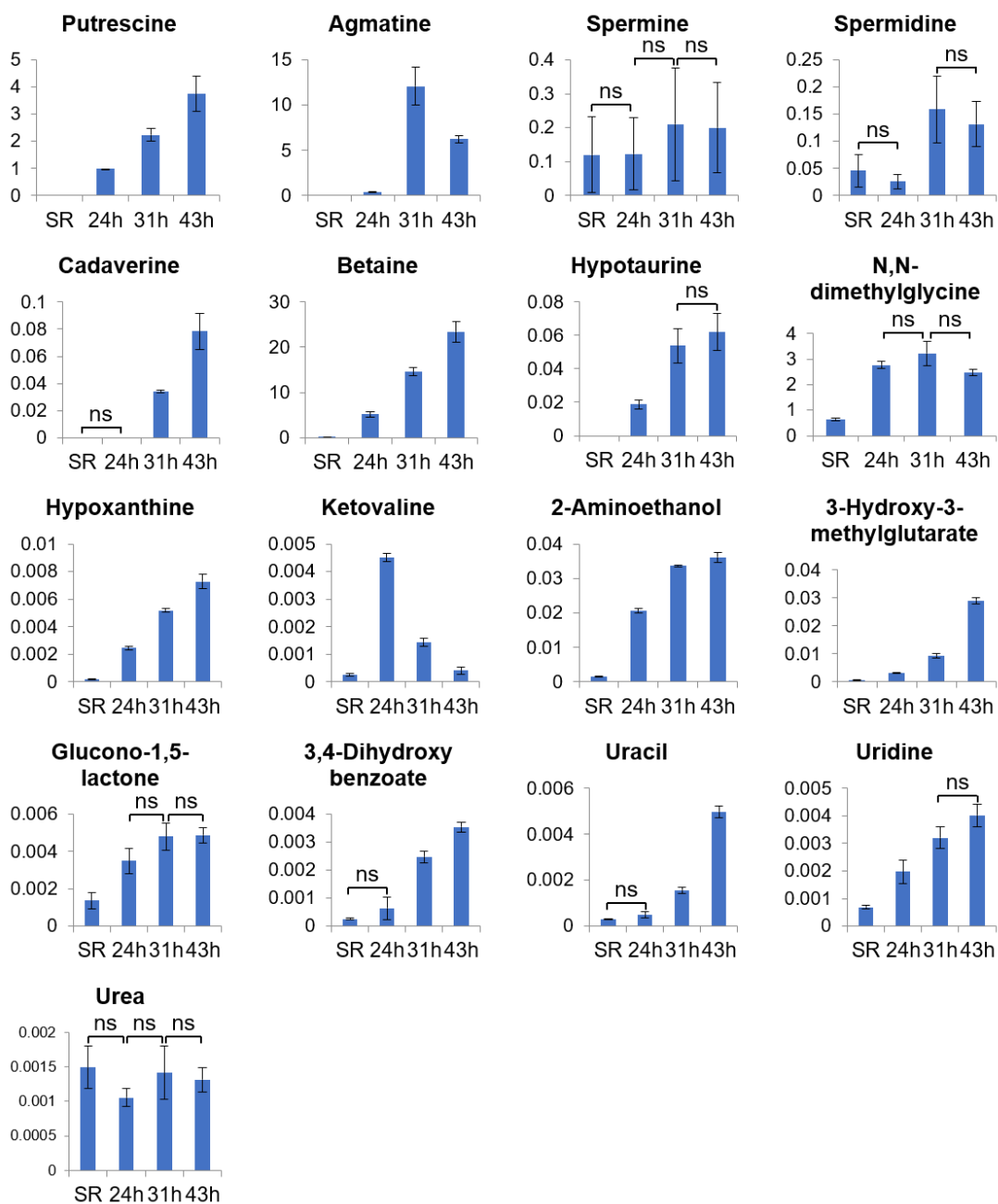


**Figure 3.6 Relative intensity of polyamines and other metabolites during rice *koji*-making. X-axis represents sampling points (SR: steamed rice), while Y-axis represents relative intensity towards the internal standard. Changes between time points are significant ( $p < 0.05$ ), unless denoted (ns).**

Other amine compounds such as polyamines were generally increased, as seen in Figure 3.6. Polyamines are known to be essential for a variety of growth and developmental events in various organisms, including fungi (Khurana et al. 1996).

Putrescine may act as a precursor for GABA as well as spermidine synthesis, which is essential for *Aspergillus* hyphal growth (Jin et al. 2002). A recent study also revealed that *A. oryzae* is the main agmatine-producing microorganism in a system including *Saccharomyces cerevisiae* (Akasaka et al. 2018). Interestingly, the production of agmatine peaked at 31-hour. On the other hand, spermine level changes are not significant ( $p>0.05$ ), agreeing with reports that it is not produced by *A. oryzae* (Akasaka et al. 2018). While there was a report about betaine detected in *amazake* (Oguro et al. 2017), there were no studies specifically stating that betaine is increased in rice *koji*. The increase of betaine may be associated with its precursor, choline, which is known to be related to hyphae branching of filamentous fungi such as *Aspergillus* (Markham et al. 1993).

Other metabolites were also shown to be increased during the rice *koji*-making process. The sharp increase of ketovaline at 24-hour, followed by the gradual decrease, may be related to the production of valine, leucine, and isoleucine, as the three amino acids were shown to peak at 31-hour. A gradual increase of glucono-1,5-lactone indicated the activity of the pentose phosphate pathway during the growth of the fungi. Uridine and uracil were increased gradually as well, possibly due to its vital role in fungal survival (Nguyen et al. 2017).

### **3.4 Conclusion**

A comprehensive time-course metabolite profiling of rice *koji* was conducted in this study. The approach successfully revealed the metabolite changes of sugars, sugar alcohols, amino acids, organic acids, polyamines, and other metabolites during rice *koji*-making. The use of LC-MS for targeted analysis of amino acids and other amine metabolites provided a more exhaustive profiling and insight into time-related changes of these amine metabolites.

The metabolite classes that were especially affected were that of sugars, sugar alcohols, amino acids, and other amines. The production of various metabolites, as well as the dynamic changes during the rice *koji*-making process from these metabolite classes, indicated that the inoculation of *A. oryzae* highly affected the characteristics of the steamed rice grain.

## Chapter 4

### Visualization of metabolites in rice *koji* made by GUS strain

#### *Aspergillus oryzae*

##### 4.1 Introduction

The metabolite changes during rice *koji*-making have been reported using various techniques, such as metabolomic profiling (Lee et al. 2018). However, they were not able to extract spatial information of the metabolites inside. Thus, it is hard to completely correlate the changes with the profile of *haze-komi*. A visualization approach for the analysis of metabolites is necessary to address this issue.

The use of mass spectrometry imaging (MSI) is promising as it is able to visualize multiple metabolites without the use of labeling techniques. The application of MSI for food imaging has been made for various purposes, such as characterization and quality evaluation of food materials (Kadam et al. 2016). This technique is suitable for investigating the metabolite changes during rice *koji*-making, as visual data is needed to compare with the profile of mycelial penetration.

In this chapter, the rice *koji* was subjected to MSI analysis to analyze the metabolite classes that were found to be highly affected based on results from chapter 3; sugars, sugar alcohols, amino acids, and other amines. The results were then compared to GUS staining results to reveal the possible correlation of *haze-komi* and metabolites distribution.

##### 4.2 Experimental

###### 4.2.1 Samples and chemicals

*Hakutsuru nishiki*-type (polishing rate 70%) steamed rice and rice *koji* made with GUS-expressing *A. oryzae* were the same samples as in chapter 3. Materials for sectioning of samples as well for GUS histochemistry were as described in the experimental section of chapter 2. Standards (sugars, sugar alcohols, amino acids, and other amine metabolites) were purchased from Fujifilm Wako Pure Chemical Corporation (Osaka, Japan), Merck & Co. Inc. (Rockville, MD, US), Nacalai Tesque, Inc. (Kyoto, Japan), or Tokyo Chemical Industry Co. Ltd. (Tokyo, Japan). For the preparation of solvents, methanol (MeOH) was purchased from Kanto Chemical Co., Inc. (Tokyo, Japan), while ultrapure water was obtained through Barnstead GenPure xCAD Plus water purification system by Thermo

Fisher Scientific (Tokyo, Japan). The matrix N-(1-Naphthyl) ethylenediamine dihydrochloride (NEDC), 2,5-dihydroxybenzoic acid (DHB), and derivatization agent for amino acid imaging 2,4-diphenyl-pyranilium tetrafluoroborate (DPP-TFB) were purchased from Merck. Triethylamine (TEA) for part of the DPP-TFB buffer was obtained from Wako.

#### 4.2.2 Sample preparation

Sample sectioning was conducted based on the experimental section in chapter 2. After acquiring serial sections of the samples on adhesive cryofilm, conductive double-sided tape (Shielding Non-woven Fabric Tape; 3M company St. Paul, MN, USA) was utilized to attach it to Indium Tin Oxide (ITO) glass slide ( $100 \Omega/\text{m}^2$  without anti-peeling coating; Matsunami Glass, Osaka, Japan). For sugar imaging, a solution of the NEDC matrix (7 mg/mL in 50% MeOH) was applied manually using an airbrush (PS-270, GSI Creos, Tokyo, Japan). For amino acid imaging, the DPP-TFB stock solution (10 mg/mL in MeOH) was first prepared. The working solution for derivatization contained 8% of the stock solution in a buffer containing MeOH, ultrapure water, and TEA (6/9/0.01, v/v/v). The samples were sprayed with the DPP-TFB working solution and incubated for 1.5 hours. The matrix DHB (50 mg/mL in 50% MeOH) was then subsequently sprayed before analysis. For other amine analysis, the sections were directly sprayed with DHB matrix.

#### 4.2.3 MALDI-IT-TOF MSI analysis

A MALDI-MSI instrument iMScope TRIO (Shimadzu, Kyoto, Japan) with Nd:YAG ( $\lambda = 355 \text{ nm}$ ) laser was used for analysis. For sugar analysis, the instrument was operated in negative mode, and spectra were acquired in the range of  $m/z$  115 to 550. One section of each sample was used for the scan analysis. For amino acid imaging, the instrument was operated in positive mode, and the fragment ion  $m/z$  232.11 were targeted for each amino acid precursor. Two serial sections of each sample were used for the targeted MS/MS analysis. Each section was used to analyze nine targeted amino acids. The area of laser shot was shifted  $10 \mu\text{m}$  to either right or downwards of the original area after each analysis. For other amine metabolites analysis, the instrument was operated in positive mode and mass spectra were acquired in the range of  $m/z$  50 to 300. Laser diameter and intensity was set to 2 (arbitrary unit; approximately  $25 \mu\text{m}$ ) and 70 (arbitrary

unit), respectively. All MSI images were acquired with a 50  $\mu\text{m}$  pitch. Acquired data were then processed using Imaging MS Solution (Shimadzu, Kyoto, Japan). For the comparison of distribution, the absolute intensity from the sample with a higher value of each metabolite was used as the high limit value for both samples.

### 4.3 Results and discussion

#### 4.3.1 Mass imaging of sugars and sugar alcohols

As mentioned in the introduction of this chapter, different types of sugars as well as sugar alcohols were targeted for MSI analysis. The NEDC matrix was utilized as it was reported to be able to visualize glucose due to the formation of  $[\text{M}+\text{Cl}]^-$  adducted ion (Wang et al. 2015). This principle was known to apply to other sugars (Boutegrabet et al. 2012). Hence, other sugars are theoretically able to be detected with the same method. However, isomers could not be separated using this method, causing some sugars that share the same  $m/z$  value to be indistinguishable. The list of sugars and sugar alcohols that were confirmed with standards can be found in Table 4.1.

The method was then applied to imaging by spraying the NEDC matrix on the sample. Sugar and sugar alcohols were all detected as  $[\text{M}+\text{Cl}]^-$  ion. There are 9 peaks detected;  $m/z$  127.02 (glycerol),  $m/z$  157.03 (erythritol, threitol),  $m/z$  185.02 (arabinose, ribose),  $m/z$  187.03 (arabitol, xylitol),  $m/z$  215.03 (fructose, glucose, inositol, sorbose),  $m/z$  217.04 (mannitol, sorbitol),  $m/z$  377.05 (gentiobiose, lactose, maltose, melibiose, sucrose, trehalose),  $m/z$  379.06, and  $m/z$  539.06 (panose, maltotriose, raffinose). The peak detected at  $m/z$  215.03 is thought to be mainly originating from glucose, as the major sugar produced by the amylolytic enzymes originating from rice *koji* is reported to be glucose (Baba et al. 1974). However, the possibility of glucose isomers also included in the distribution profile of  $m/z$  215.03 should be acknowledged. The ion distribution can be found in Figure 4.1.

**Table 4.1 List of sugars and sugar alcohols detected in MSI analysis**

<b>No</b>	<b>Name</b>	<b>Theoretical MW</b>	<b>Theoretical <math>m/z</math> after Cl ion adduct</b>	<b>Detected <math>m/z</math> value</b>
1	Glycerol	92.09	126.95	127.02
2	Meso erythritol	122.12	156.98	157.03
3	Threitol	122.12	156.98	
4	Arabinose	150.13	184.99	185.02
5	Ribose	150.13	184.99	
6	Arabitol	152.14	187.00	187.03
7	Xylitol	152.15	187.01	
8	Fructose	180.16	215.02	215.03
9	Glucose	180.16	215.02	
10	Inositol	180.16	215.02	
11	Sorbose	180.16	215.02	
12	Mannitol	182.17	217.03	217.04
13	Sorbitol	182.17	217.03	
14	Gentiobiose	342.30	377.16	377.05
15	Lactose	342.30	377.16	
16	Maltose	342.30	377.16	
17	Melibiose	342.30	377.16	
18	Sucrose	342.30	377.16	
19	Trehalose	342.30	377.16	
20	Lactitol	344.31	379.17	379.06
21	Panose	504.44	539.30	539.06
22	Maltotriose	504.44	539.30	
23	Raffinose	504.42	539.28	

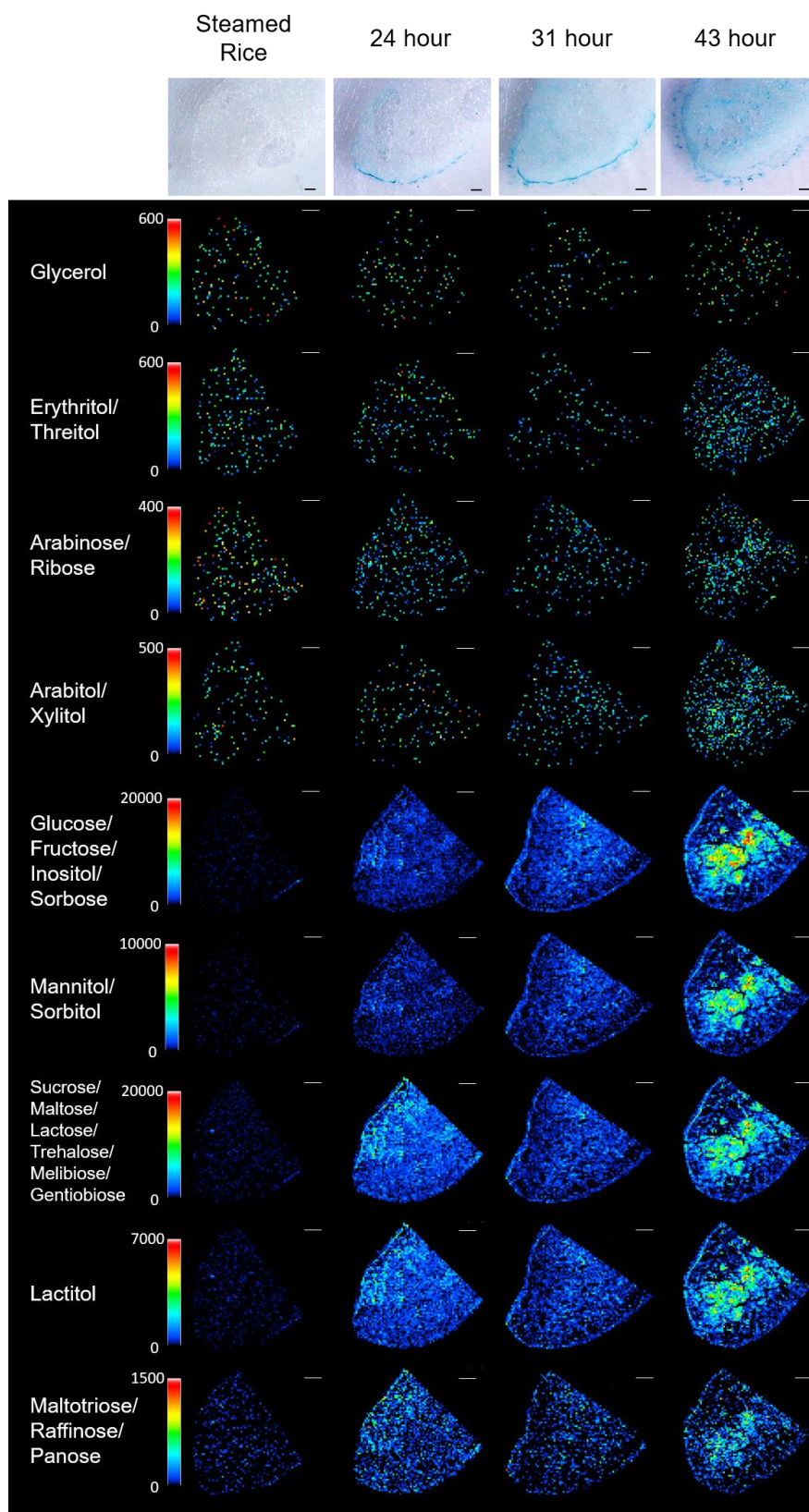


**Figure 4.1 Ion distribution of sugars and sugar alcohols during rice *koji*-making. Intensity is denoted in the rainbow scale for each metabolite. Scale bar is 500 μm.**

All of the sugar and sugar alcohols showed a change in distribution during rice *koji*-making. Most of the peaks were barely detected from steamed rice. By the 24-hour time point, the sugars and sugar alcohols were evenly distributed on the cross-section of rice *koji*. The same trend can be seen at the 31-hour time point, with slightly more accumulation in the middle part. At the end of the process, accumulation can be clearly seen in the middle of the rice *koji* grain.

Compared with the *haze-komi* profile in each time point, the distribution of the sugar metabolites does not seem to correlate directly to the position of mycelia. At 24-hour, the mycelia can be seen shallowly penetrating the steamed rice. However, the sugars and sugar alcohols are already evenly distributed. While accumulation can be seen at 31- and 43-hour time point, the position was in the center of the grain. The even distribution of sugars from 24-hour time point may suggest that the secreted amyolytic enzymes were also distributed evenly.

#### **4.3.2 Mass imaging of amino acids**

In amino acid imaging, derivatization agent DPP-TFB was applied before matrix application. On-tissue detection of amino metabolites has been known to be difficult due to the low-ionization efficiency and spectral interferences from the MALDI matrix. Thus, the use of on-tissue derivatization is one of the methods to increase the detectability of amino metabolites (Esteve et al. 2016). However, several amino acids with isomers such as leucine and isoleucine were not able to be separated using this method. The list of detectable amino acids can be found in Table 4.2.

**Table 4.2 List of amino acids detected in MSI analysis**

No	Name	Theoretical MW	Theoretical <i>m/z</i> after DPP-TFB derivatization
1	Glycine	75.07	290.16
2	Alanine	89.09	304.18
3	GABA	103.12	318.21
4	Serine	105.09	320.18
5	Proline	115.13	330.22
6	Valine	117.15	332.24
7	Threonine	119.12	334.21
8	Cysteine	121.06	336.15
9	Isoleucine	131.17	346.26
10	Leucine	131.17	
11	Asparagine	132.12	347.21
12	Aspartic acid	133.11	348.20
13	Lysine	146.11	361.20
14	Glutamine	146.14	
15	Glutamic acid	147.13	362.22
16	Histidine	155.08	370.17
17	Phenylalanine	165.19	380.28
18	Arginine	174.12	389.21
19	Tyrosine	181.19	396.28
20	Tryptophan	204.23	419.32

Derivatized amino acids were detected through MS/MS analysis as *m/z* 232.11 after fragmentation of the parent ions. There are 18 peaks detected; *m/z* 290.16 (glycine), *m/z* 304.18 (alanine), *m/z* 318.21 (GABA), *m/z* 320.18 (serine), *m/z* 330.22 (proline), *m/z* 332.24 (valine), *m/z* 334.21 (threonine), *m/z* 336.15 (cysteine), *m/z* 346.26 (leucine, isoleucine), *m/z* 347.21 (asparagine), *m/z* 348.20 (aspartic acid), *m/z* 361.20 (lysine, glutamine), *m/z* 362.22 (glutamic acid), *m/z* 370.17 (histidine), *m/z* 380.28 (phenylalanine), *m/z* 389.21 (arginine), *m/z* 396.28 (tyrosine), and *m/z* 419.32 (tryptophan). The ion distributions are visualized in Figure 4.2 and 4.3.

In general, all amino acids detected with MSI exhibited similar increasing trend with the result of metabolite profiling. A careful observation at 24-hour time point revealed that the distribution profile differed into two patterns. The first pattern exhibited accumulation near the surface (GABA, serine, cysteine, leucine/isoleucine, asparagine,

aspartic acid, lysine/glutamine, glutamic acid, phenylalanine, arginine, tyrosine, tryptophan), while other amino acids (glycine, alanine, proline, valine, threonine, histidine) were distributed evenly on the cross-section. The distribution profile then altered at 31-hour, where most of the amino acids were evenly distributed inside the rice *koji*. An exception was seen for cysteine, which still accumulated mostly around the surface, and tyrosine, which exhibited slight accumulation in the middle part of the grain. By the end of the *koji*-making process at 43-hour, the distribution of amino acids displayed a similar pattern of accumulation in an area between the surface and center of the grain. An exception was once again observed for cysteine and tyrosine with a profile similar to the previous time point. Another exception could be considered from the observation of histidine, phenylalanine, and tryptophan, where they seem to exhibit an even distribution across the section. This result was in contrast with the assumption that all amino acids would exhibit the same distribution profile. A previous study reported that higher polishing rate resulted in the simultaneous decrease of various amino acid content in rice *koji* (Iwano et al. 2004), which would imply that the amino acids would have similar distribution pattern. The current approach was unable to determine why the distributions of some amino acids were different from the others. Nonetheless, this finding would not be obtained without the use of imaging techniques.

Comparison with the GUS-stained sections revealed that the amino acids distribution seems to correlate with the *haze-komi* profile. As stated before, most of the amino acids at the 24-hour time point showed accumulation near the surface of the grain. Furthermore, the accumulation was especially close to the position of the indigo-stained area, which indicates the presence of mycelia. When the mycelia have covered the whole grain at the 31-hour time point, the distribution of amino acids was also shown to be even. The correlation suggested that the protease and peptidase were not distributed in a similar manner with amylolytic enzymes at 24-hour time point.

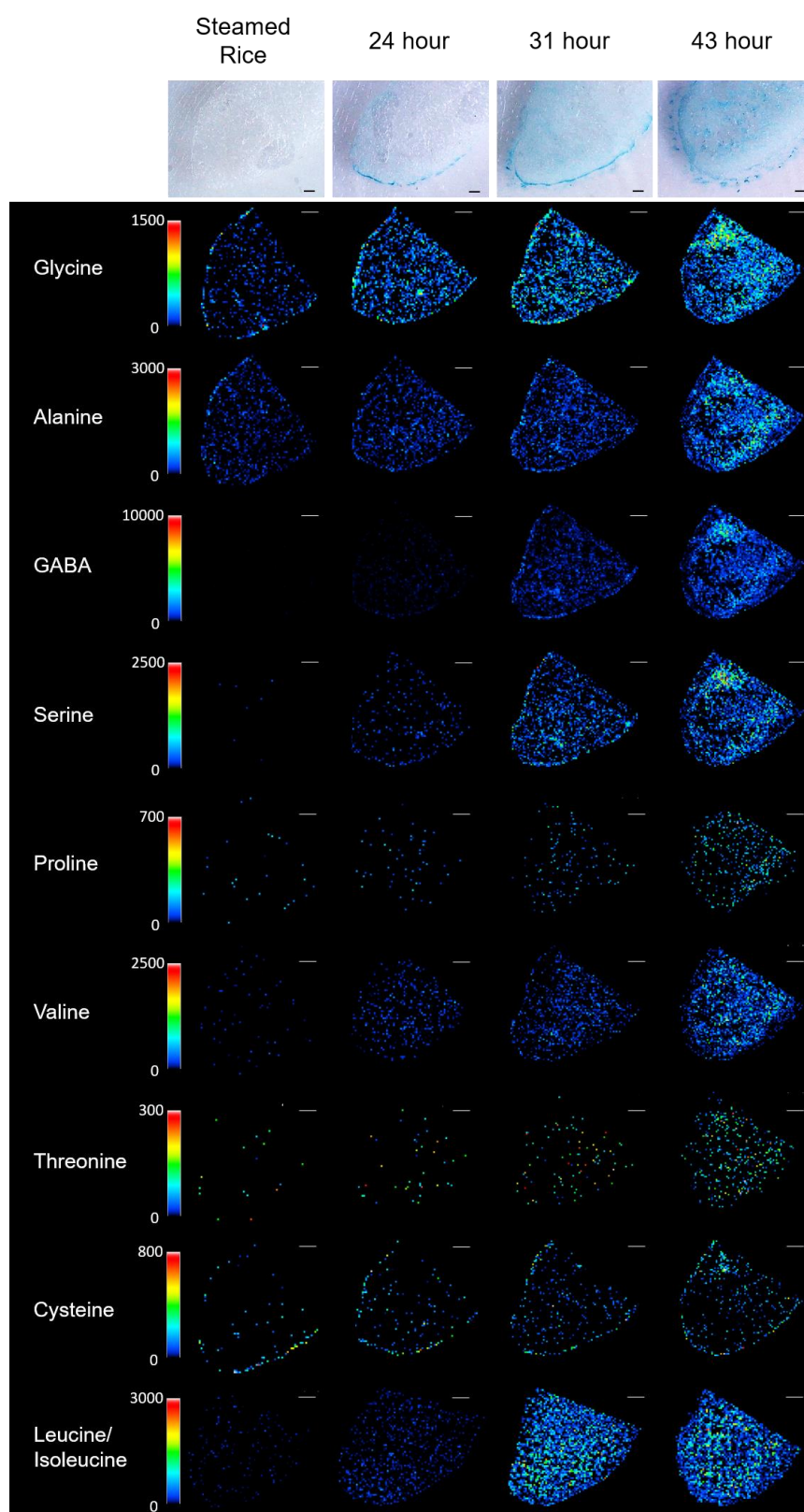


**Figure 4.2 Ion distribution of amino acids during rice *koji*-making. Intensity is denoted in the rainbow scale for each metabolite. Scale bar is 500  $\mu$ m.**

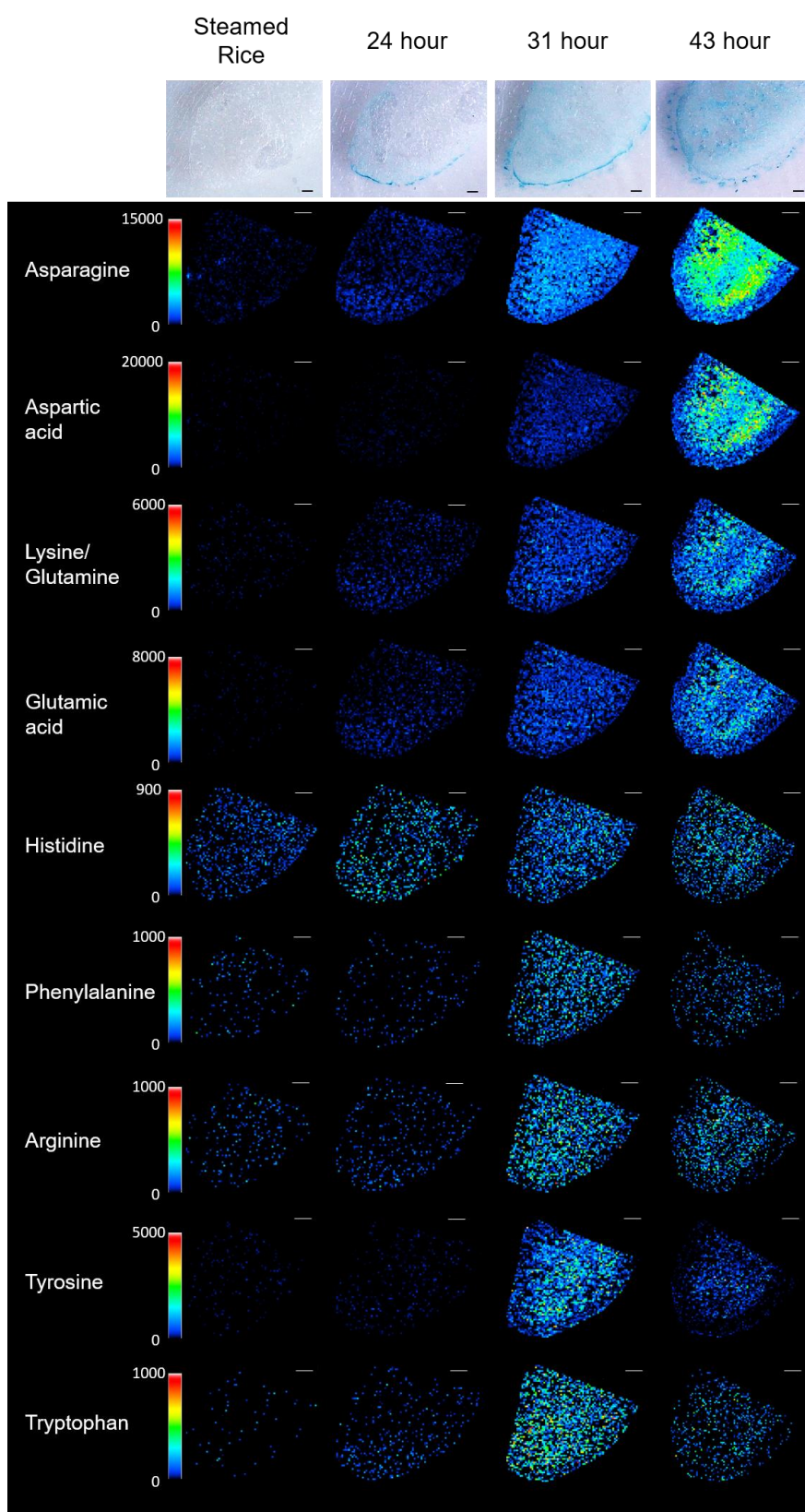


**Figure 4.3 Ion distribution of amino acids during rice *koji*-making (cont'd). Intensity is denoted in the rainbow scale for each metabolite. Scale bar is 500 μm.**

### 4.3.3 Mass imaging of other amine metabolites

The matrix DHB was used for other amine metabolites imaging, as a previous study has proved the ability of this matrix to detect spermine and spermidine (Sagara et al. 2020). The detected metabolites are listed in Table 4.3.

**Table 4.3 List of other amine metabolites detected in MSI analysis**

No	Name	Theoretical MW	Theoretical $m/z$	Detected $m/z$ value
1	Putrescine	88.15	89.15	89.11
2	Cadaverine	102.18	103.18	103.12
3	Betaine	117.15	118.15	118.09
4	Agmatine	130.19	131.19	131.13
5	Spermidine	145.25	146.25	146.17
6	Spermine	202.34	203.34	203.22

From the imaging result, polyamines displayed various patterns of distribution, as seen in Figure 4.4. Putrescine and cadaverine seem to be evenly distributed across the section of rice *koji* on all time points. Agmatine showed a tendency on an area near the center of rice *koji* at 31-hour time point. Meanwhile, spermidine exhibited accumulation on the surface of rice *koji* at 31-hour time point. The accumulation of spermidine on the surface at 31-hour might be related to its importance for the developmental transitions of *Aspergillus* (Jin et al. 2002). Spermine was accumulated on the surface of steamed rice. However, it was hardly detected after the process of rice *koji*-making. On the other hand, betaine was mainly accumulated below the surface towards the center of the grain. This trend can be observed from 24-hour to the 43-hour time point.

The spatial distribution of each metabolite was then compared with the *haze-komi* profile at each time point. Overall, a pattern that correlated with the position of mycelia cannot be found at the 24-hour time point, as most metabolites were distributed evenly across the section. The same trend can be seen at 31-hour and 43-hour time point. This may imply that the *haze-komi* profile does not correlate with the distribution of other amine metabolites. However, it should be noted that the intensity of the detected polyamines was very low, making it hard to observe the true distribution. Improvement of polyamine imaging should be considered in the future.

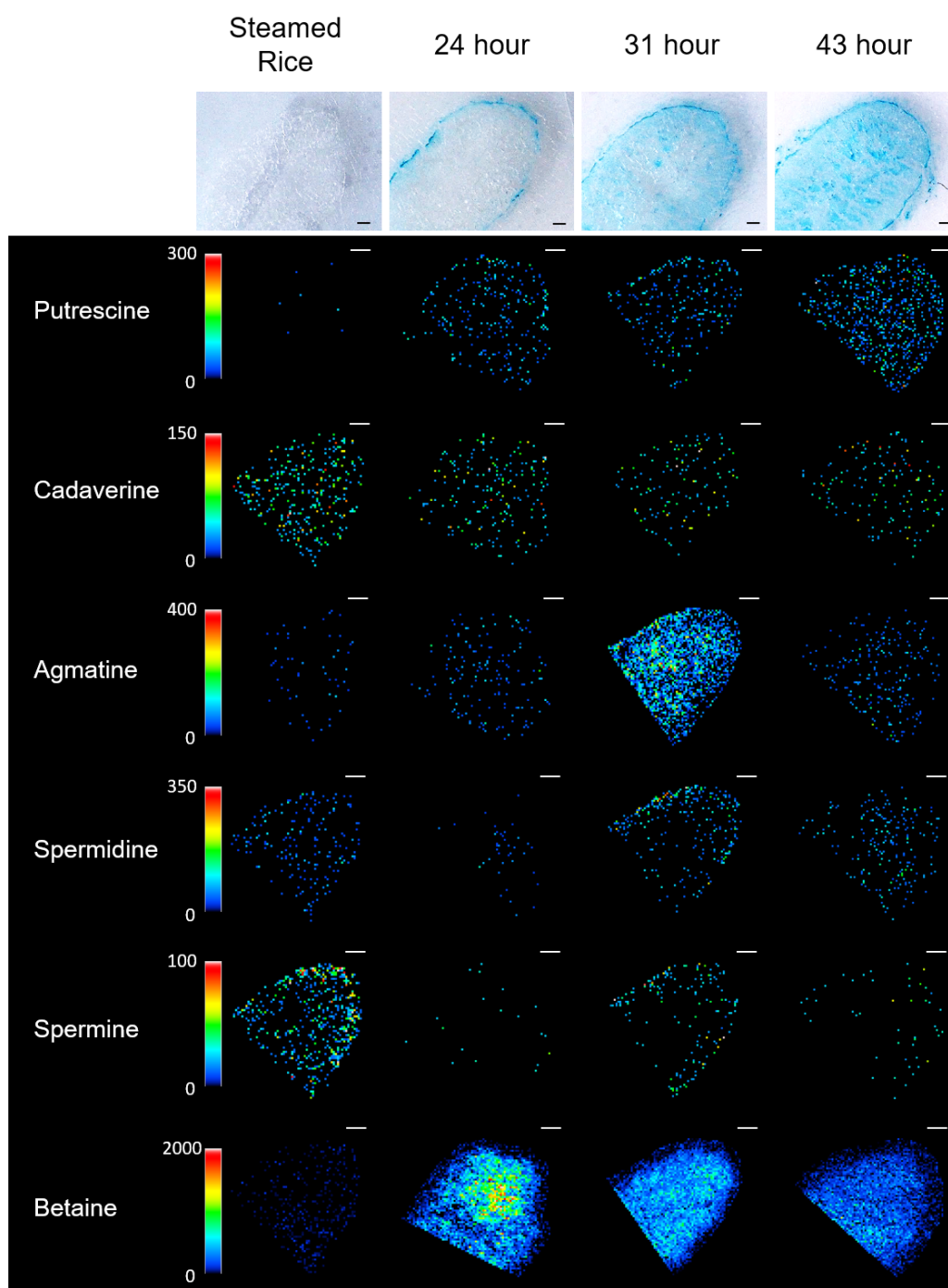


**Figure 4.4 Ion distribution of polyamines and betaine during rice *koji*-making. Intensity is denoted in rainbow scale for each metabolite. Scale bar is 500  $\mu$ m.**

#### 4.4 Conclusion

Metabolite imaging of sugars, sugar alcohols, amino acids, and other amine metabolites was conducted in this chapter. Visual observation revealed distinct distributions between each metabolite classes. Sugars and sugar alcohols were mainly distributed evenly during the course of rice *koji*-making, leading to accumulation in the center of the grain at the end of the process. Amino acids displayed a more variative pattern contrary to assumptions, with difference observed mainly at 24- and 43-hour time points. Other amine metabolites also exhibited different trends depending on the observed metabolite.

By comparing the distribution of metabolites to the *haze-komi* profile on each time point, the correlation tendency for each metabolite classes can be concluded. In general, sugars and sugars alcohols distribution did not seem to be correlated with mycelial penetration. The spatial distribution of other amine metabolites was also found to be independent of the *haze-komi* profile. On the other hand, amino acid distribution, especially at the 24-hour time point, were correlated with the position of mycelia.

## Chapter 5

### Conclusion and Future Perspective

#### 5.1 Conclusion

In this thesis, the combination of metabolomics and imaging techniques successfully accumulated knowledge about the trend of *haze-komi* and metabolites alteration during the rice *koji*-making process. GUS histochemistry was applied for the observation of *haze-komi* on a thin section and could clearly map the progression of mycelial penetration. The fungi shallowly penetrated steamed rice at 24-hour time point before completely covering the whole grain. The metabolite alteration was profiled by comprehensive time-course metabolite profiling employing GC- and LC-MS, revealing the changes of sugars, sugar alcohols, amino acids, organic acids, polyamines, and other metabolites during rice *koji*-making. The use of MSI successfully visualized the several classes of metabolites found from metabolomics analysis. An unexpected result was found for the distribution profile of amino acids, where they have various distribution pattern mainly at 24- and 43-hour time points. Furthermore, this approach enabled a correlation study between the *haze-komi* profile and the metabolites distribution, where the correlation depended on the class of metabolite. Sugars, sugar alcohols, and amine metabolites did not seem to correlate with *haze-komi*, while amino acids correlated with the *haze-komi* progression.

#### 5.2 Future perspective

As mentioned in chapter 1, rice *koji* is considered as an important material for the food and beverage industry. Much effort was done to improve the rice *koji* quality in the industry. However, the improvement was based mainly on trial and error, which is considered inefficient. This is due to the lack of knowledge regarding the events or mechanisms that occurs during rice *koji*-making process. There is a demand from the industry, especially *sake* industry, for the research related to rice *koji*-making involving various approaches and technology. MSI and histochemistry as a visualization method can facilitate the study to understand the underlying mechanism.

The presented approach is applicable for further investigation or studies related to *haze-komi* and metabolites distribution. The investigation of different types of *haze*, such as *tsuki-haze* and *sou-haze*, and its relation to rice *koji* quality would be a suitable

application for this approach. The NRIB has described that each type of *haze* gave a different enzymatic profile. A metabolomic study would provide more thorough information on the effect of *haze* on rice *koji* quality. Studies of factors related to *haze-komi* could also be pursued, such as the effect of rice moisture content. Previous studies have investigated the relation between *haze-komi* and rice moisture content (Sudo et al. 2002; Matsuyama 1964). However, an additional observation from the metabolomic approach may give more insight into the issue and could become a material of consideration for rice *koji*-making protocol.

Additionally, the different distribution profile between sugars and amino acids may suggest the different distribution of the amylolytic enzymes and the protease or peptidase. The visualization of the enzyme distribution changes would give more information regarding this hypothesis.

## References

- Akasaka, N., Kato, S., Kato, S., Hidese, R., Wagu, Y., Sakoda, H., Fujiwara, S.:** Agmatine production by *Aspergillus oryzae* is elevated by low pH during solid-state cultivation. C. A. Elkins, ed. *Appl. Environ. Microbiol.*, **84**, 1–17 Available at: <http://aem.asm.org/lookup/doi/10.1128/AEM.00722-18>.(2018).
- Aretz, I., Meierhofer, D.:** Advantages and pitfalls of mass spectrometry based metabolome profiling in systems biology. *Int. J. Mol. Sci.*, **17** (2016).
- Baba, S., Oguri, I., Fukuzawa, M., Iida, T., Kobayashi, I., Imai, K.:** Oligosaccharide production by *koji-kin* enzymes. *J. Brew. Soc. Japan*, **69**, 781–783 Available at: <http://joi.jlc.jst.go.jp/JST.Journalarchive/jbrewsocjapan1915/69.781?from=CrossRef>.(1974).
- Te Biesebeke, R., Ruijter, G., Rahardjo, Y.S.P., Hoogschagen, M.J., Heerikhuisen, M., Levin, A., Van Driel, K.G.A., Schutyser, M.A.I., Dijksterhuis, J., Zhu, Y., Weber, F.J., De Vos, W.M., Van Den Hondel, K.A.M.J.J., Rinzema, A., Punt, P.J.:** *Aspergillus oryzae* in solid-state and submerged fermentations: Progress report on a multi-disciplinary project. *FEMS Yeast Res.*, **2**, 245–248 (2002).
- Bjarnholt, N., Li, B., D’Alvise, J., Janfelt, C.:** Mass spectrometry imaging of plant metabolites – principles and possibilities. *Nat. Prod. Rep.*, **31**, 818–837 Available at: <http://xlink.rsc.org/?DOI=C3NP70100J>.(2014).
- Boutegrabet, L., Kanawati, B., Gebefügi, I., Peyron, D., Cayot, P., Gougeon, R.D., Schmitt-Kopplin, P.:** Attachment of chloride anion to sugars: Mechanistic investigation and discovery of a new dopant for efficient sugar ionization/detection in mass spectrometers. *Chem. - A Eur. J.*, **18**, 13059–13067 (2012).
- Breil, C., Abert Vian, M., Zemb, T., Kunz, W., Chemat, F.:** “Bligh and Dyer” and Folch methods for solid–liquid–liquid extraction of lipids from microorganisms. Comprehension of solvation mechanisms and towards substitution with alternative solvents. *Int. J. Mol. Sci.*, **18**, 1–21 (2017).
- Brown, R.L., Cleveland, T.E., Payne, G.A., Woloshuk, C.P., White, D.G.:** Growth of an *Aspergillus flavus* transformant expressing *Escherichia coli*  $\beta$ -glucuronidase in maize kernels resistant to aflatoxin production. *J. Food Prot.*, **60**, 84–87 (1997).
- Canela, N., Rodríguez, M.Á., Baiges, I., Nadal, P., Arola, L.:** Foodomics imaging by mass spectrometry and magnetic resonance. *Electrophoresis*, **37**, 1748–1767 Available at: <http://doi.wiley.com/10.1002/elps.201500494>.(2016).
- Caprioli, R.M., Farmer, T.B., Gile, J.:** Molecular imaging of biological samples: localization of peptides and proteins using MALDI-TOF MS. *Anal. Chem.*, **69**, 4751–4760 (1997).
- Dave, K.K., Punekar, N.S.:** Expression of lactate dehydrogenase in *Aspergillus niger* for L-lactic acid production. *PLoS One*, **10**, 1–16 (2015).
- Dong, Y., Li, B., Malitsky, S., Rogachev, I., Aharoni, A., Kaftan, F., Svatoš, A., Franceschi, P.:** Sample preparation for mass spectrometry imaging of plant tissues:

a review. *Front. Plant Sci.*, **7**, 60 Available at: <http://www.pubmedcentral.nih.gov/articlerender.fcgi?artid=4748743&tool=pmcentrez&rendertype=abstract>.(2016).

- Esteve, C., Tolner, E.A., Shyti, R., van den Maagdenberg, A.M.J.M., McDonnell, L.A.:** Mass spectrometry imaging of amino neurotransmitters: a comparison of derivatization methods and application in mouse brain tissue. *Metabolomics*, **12**, 1–9 (2016).
- Fujii, F., Ozeki, K., Kanda, A., Hamachi, M., Nunokawa, Y.:** A simple method for the determination of grown mycelial content in rice *koji* using commercial cell wall lytic enzyme, yatalase. *J. Brew. Soc. Japan*, **87**, 757–759 Available at: [https://www.jstage.jst.go.jp/article/jbrewsocjapan1988/87/10/87\\_10\\_757/\\_article](https://www.jstage.jst.go.jp/article/jbrewsocjapan1988/87/10/87_10_757/_article).(1992).
- Fujino, Y., Minamizaki, T., Yoshioka, H., Okada, M., Yoshiko, Y.:** Imaging and mapping of mouse bone using MALDI-imaging mass spectrometry. *Bone Reports*, **5**, 280–285 Available at: <http://dx.doi.org/10.1016/j.bonr.2016.09.004>.(2016).
- Fujita, H., Yamane, Y.I., Fukuda, H., Kizaki, Y., Wakabayashi, S., Shigeta, S., Suzuki, O., Ono, K.:** Production and properties of phytase and acid phosphatase from a *sake koji* mold, *Aspergillus oryzae*. *J. Biosci. Bioeng.*, **95**, 348–353 (2003).
- Gomi, K., Iimura, Y., Hara, S.:** Integrative transformation of *Aspergillus oryzae* with a plasmid containing the *Aspergillus nidulans argB* gene. *Agric. Biol. Chem.*, **51**, 2549–2555 Available at: <http://www.tandfonline.com/doi/full/10.1080/00021369.1987.10868429>.(1987).
- Gottschalk, T.E., Nielsen, J.E., Rasmussen, P.:** Detection of endogenous  $\beta$ -glucuronidase activity in *Aspergillus niger*. *Appl. Microbiol. Biotechnol.*, **45**, 240–244 (1996).
- Halket, J.M., Waterman, D., Przyborowska, A.M., Patel, R.K.P., Fraser, P.D., Bramley, P.M.:** Chemical derivatization and mass spectral libraries in metabolic profiling by GC/MS and LC/MS/MS. *J. Exp. Bot.*, **56**, 219–243 (2005).
- Handberg, E., Chingin, K., Wang, N., Dai, X., Chen, H.:** Mass spectrometry imaging for visualizing organic analytes in food. *Mass Spectrom. Rev.*, **34**, 641–658 (2015).
- Hankin, J.A., Barkley, R.M., Murphy, R.C.:** Sublimation as a method of matrix application for mass spectrometric imaging. *J. Am. Soc. Mass Spectrom.*, **18**, 1646–1652 (2007).
- Harada, R., Yuzuki, M., Ito, K., Shiga, K., Bamba, T., Fukusaki, E.:** Influence of yeast and lactic acid bacterium on the constituent profile of soy sauce during fermentation. *J. Biosci. Bioeng.*, **123**, 203–208 (2017).
- Ito, K., Gomi, K., Kariyama, M., Miyake, T.:** Quantitative evaluation of *haze* formation of *koji* and progression of internal *haze* by drying of *koji* during *koji* making. *J. Biosci. Bioeng.*, **124**, 62–70 Available at: <http://dx.doi.org/10.1016/j.jbiosc.2017.02.011>.(2016).

- Ito, K., Kimizuka, A., Okazaki, N., Kobayashi, S.:** Mycelial distribution in rice *koji*. *J. Ferment. Bioeng.*, **68**, 7–13 (1989).
- Ito, K., Yoshida, K., Ishikawa, T., Kobayashi, S.:** Volatile compounds produced by the fungus *Aspergillus oryzae* in rice *koji* and their changes during cultivation. *J. Ferment. Bioeng.*, **70**, 169–172 (1990).
- Ito, T., Takahashi, H., Shiga, T., Sato, T., Nakazawa, N., Iwano, K.:** Analysis of the amino acid content of *sake koji* and estimation of the amino acid amount formed by *Aspergillus oryzae* in *sake koji* making. *J. Brew. Soc. Japan*, **108**, 453–460 Available at: [https://www.jstage.jst.go.jp/article/jbrewsocjapan/108/6/108\\_453/\\_article](https://www.jstage.jst.go.jp/article/jbrewsocjapan/108/6/108_453/_article).(2013).
- Iwano, K., Ito, T., Hasegawa, E., Takahashi, K., Takahashi, H., Nakazawa, N.:** Influence of the variety of rice and polishing rate on Japanese *sake koji* making. *J. Brew. Soc. Japan*, **99**, 55–63 Available at: [https://www.jstage.jst.go.jp/article/jbrewsocjapan1988/99/1/99\\_1\\_55/\\_article](https://www.jstage.jst.go.jp/article/jbrewsocjapan1988/99/1/99_1_55/_article).(2004).
- Iwano, K., Nakazawa, N., Ito, T.:** The relation between the growth of *Aspergillus oryzae* and metabolism products in *sake koji*. *J. Soc. Brew.*, **97**, 865–871 Available at: [https://www.jstage.jst.go.jp/article/jbrewsocjapan1988/97/12/97\\_12\\_865/\\_article](https://www.jstage.jst.go.jp/article/jbrewsocjapan1988/97/12/97_12_865/_article).(2002).
- Jefferson, R.A., Kavanagh, T.A., Bevan, M.W.:** GUS fusions:  $\beta$ -glucuronidase as a sensitive and versatile gene fusion marker in higher plants. *EMBO J.*, **6**, 3901–7 Available at: <http://www.ncbi.nlm.nih.gov/pubmed/3327686> <http://www.pubmedcentral.nih.gov/articlerender.fcgi?artid=PMC553867>.(1987).
- Ji, T., Kang, M., Baik, B.K.:** Volatile organic compounds of whole-grain soft winter wheat. *Cereal Chem.*, **94**, 594–601 (2017).
- Jin, Y., Bok, J.W., Guzman-De-Peña, D., Keller, N.P.:** Requirement of spermidine for developmental transitions in *Aspergillus nidulans*. *Mol. Microbiol.*, **46**, 801–812 (2002).
- Kadam, S.U., Misra, N.N., Zaima, N.:** Mass spectrometry based chemical imaging of foods. *RSC Adv.*, **6**, 33537–33546 Available at: <http://xlink.rsc.org/?DOI=C6RA02269C>.(2016).
- Kawamoto, T.:** Use of a new adhesive film for the preparation of multi-purpose fresh-frozen sections from hard tissues, whole-animals, insects and plants. *Arch. Histol. Cytol.*, **66**, 123–143 (2003).
- Khurana, N., Saxena, R.K., Gupta, R., Rajam, M. V.:** Polyamines as modulators of microcycle conidiation in *Aspergillus flavus*. *Microbiology*, **142**, 517–523 (1996).
- Kim, A.J., Choi, J.N., Kim, J., Park, S.B., Yeo, S.H., Choi, J.H., Lee, C.H.:** GC-MS based metabolite profiling of rice *koji* fermentation by various fungi. *Biosci. Biotechnol. Biochem.*, **74**, 2267–2272 (2010).

- Kojima, H., Hasegawa, H., Magarifuchi, T., Fukuda, H.:** Observation of rice *koji* by confocal laser scanning microscopy. *Seibutsu-kogaku Kaishi*, **77**, 339–344 (1999).
- Krijghsheld, P., Bleichrodt, R., van Veluw, G.J., Wang, F., Müller, W.H., Dijksterhuis, J., Wösten, H.A.B.:** Development in *Aspergillus*. *Stud. Mycol.*, **74**, 1–29 Available at: <http://linkinghub.elsevier.com/retrieve/pii/S016606161460083X>.(2013).
- Lee, D., Lee, S., Jang, E., Shin, H., Moon, B., Lee, C.:** Metabolomic profiles of *Aspergillus oryzae* and *Bacillus amyloliquefaciens* during rice *koji* fermentation. *Molecules*, **21**, 773–787 Available at: <http://www.mdpi.com/1420-3049/21/6/773>.(2016).
- Lee, S., Lee, D.E., Singh, D., Lee, C.H.:** Metabolomics reveal optimal grain pre-processing (milling) toward rice *koji* fermentation. *J. Agric. Food Chem.*, **acs.jafc.7b05131** Available at: <http://pubs.acs.org/doi/10.1021/acs.jafc.7b05131>.(2018).
- Leopold, J., Popkova, Y., Engel, K.M., Schiller, J.:** Recent developments of useful MALDI matrices for the mass spectrometric characterization of lipids. *Biomolecules*, **8** (2018).
- Markham, P., Robson, G.D., Bainbridge, B.W., Trinci, A.P.J.:** Choline: Its role in the growth of filamentous fungi and the regulation of mycelial morphology. *FEMS Microbiol. Lett.*, **104**, 287–300 (1993).
- Matsunaga, K., Furukawa, K., Hara, S.:** Effects of enzyme activity on the mycelial penetration of rice *koji*. *J. Brew. Soc. Japan*, **97**, 721–726 (2002).
- Matsuyama, M.:** Regarding *hazekomi* in rice *koji*. *J. Soc. Brew.*, **59**, 672–675 Available at: [https://www.jstage.jst.go.jp/article/jbrewsocjapan1915/59/8/59\\_8\\_672/\\_article/-char/ja/](https://www.jstage.jst.go.jp/article/jbrewsocjapan1915/59/8/59_8_672/_article/-char/ja/).(1964).
- McDonnell, L.A., Corthals, G.L., Willems, S.M., van Remoortere, A., van Zeijl, R.J.M., Deelder, A.M.:** Peptide and protein imaging mass spectrometry in cancer research. *J. Proteomics*, **73**, 1921–1944 Available at: <http://dx.doi.org/10.1016/j.jprot.2010.05.007>.(2010).
- Nakano, Y., Taniguchi, M., Fukusaki, E.:** High-sensitive liquid chromatography-tandem mass spectrometry-based chiral metabolic profiling focusing on amino acids and related metabolites. *J. Biosci. Bioeng.*, **127**, 520–527 Available at: <https://doi.org/10.1016/j.jbiosc.2018.10.003>.(2019).
- Nguyen, K.T., Ho, Q.N., Do, L.T.B.X., Mai, L.T.D., Pham, D.N., Tran, H.T.T., Le, D.H., Nguyen, H.Q., Tran, V.T.:** A new and efficient approach for construction of uridine/uracil auxotrophic mutants in the filamentous fungus *Aspergillus oryzae* using *Agrobacterium tumefaciens*-mediated transformation. *World J. Microbiol. Biotechnol.*, **33**, 1–11 (2017).
- Oda, K., Kakizono, D., Yamada, O., Iefuji, H., Akita, O., Iwashita, K.:** Proteomic analysis of extracellular proteins from *Aspergillus oryzae* grown under submerged and solid-state culture conditions. *Appl. Environ. Microbiol.*, **72**, 3448–3457 Available at: <http://aem.asm.org/cgi/doi/10.1128/AEM.72.5.3448->

3457.2006.(2006).

- Oguro, Y., Nishiwaki, T., Shinada, R., Kobayashi, K., Kurahashi, A.:** Metabolite profile of *koji amazake* and its lactic acid fermentation product by *Lactobacillus sakei* UONUMA. *J. Biosci. Bioeng.*, **124**, 178–183 Available at: <http://dx.doi.org/10.1016/j.jbiosc.2017.03.011>.(2017).
- Oliver, R.P., Farman, M.L., Jones, J.D.G., Hammond-Kosack, E.:** Use of fungal transformants expressing  $\beta$ -glucuronidase activity to detect infection and measure hyphal biomass in infected plant tissue. *Mol. Plant-Microbe Interact.*, **6**, 521–525 (1993).
- Pongsuwan, W., Fukusaki, E., Bamba, T., Yonetani, T., Yamahara, T., Kobayashi, A.:** Prediction of Japanese green tea ranking by gas chromatography/mass spectrometry-based hydrophilic metabolite fingerprinting. *J. Agric. Food Chem.*, **55**, 231–236 (2007).
- Roberts, I.N., Oliver, R.P., Punt, P.J., Van Den Hondel, C.A.M.J.J.:** Expression of the *Escherichia coli*  $\beta$ -glucuronidase gene in industrial and phytopathogenic filamentous fungi. *Curr. Genet.*, **15**, 177–180 (1989).
- Ruijter, G.J.G., Visser, J., Rinzema, A.:** Polyol accumulation by *Aspergillus oryzae* at low water activity in solid-state fermentation. *Microbiology*, **150**, 1095–1101 (2004).
- Sagara, T., Bhandari, D.R., Spengler, B., Vollmann, J.:** Spermidine and other functional phytochemicals in soybean seeds: Spatial distribution as visualized by mass spectrometry imaging. *Food Sci. Nutr.*, **8**, 675–682 (2020).
- Sudo, S., Koseki, T., Kizaki, Y.:** Factors in the formation of *haze*. *J. Brew. Soc. Japan*, **97**, 369–376 (2002).
- Sugiura, Y., Shimma S, Setou, M.:** Thin sectioning improves the peak intensity and signal-to-noise ratio in direct tissue mass spectrometry. *J. Mass Spectrom. Soc. Jpn.*, **54**, 45–48 Available at: <https://doi.org/10.5702/massspec.54.45>.(2006).
- Tsuboi, H., Koda, A., Toda, T., Minetoki, T., Hirotsune, M., Machida, M.:** Improvement of the *Aspergillus oryzae* enolase promoter (P-enoA) by the introduction of cis-element repeats. *Biosci. Biotechnol. Biochem.*, **69**, 206–8 Available at: <http://www.ncbi.nlm.nih.gov/pubmed/15665487>.(2005).
- Tsugawa, H., Cajka, T., Kind, T., Ma, Y., Higgins, B., Ikeda, K., Kanazawa, M., Vandergheynst, J., Fiehn, O., Arita, M.:** MS-DIAL: Data-independent MS/MS deconvolution for comprehensive metabolome analysis. *Nat. Methods*, **12**, 523–526 (2015).
- Veličković, D., Ropartz, D., Guillon, F., Saulnier, L., Rogniaux, H.:** New insights into the structural and spatial variability of cell-wall polysaccharides during wheat grain development, as revealed through MALDI mass spectrometry imaging. *J. Exp. Bot.*, **65**, 2079–2091 (2014).
- Vickerman, J.C.:** Molecular imaging and depth profiling by mass spectrometry--SIMS, MALDI or DESI? *Analyst*, **136**, 2199–2217 (2011).

- Wang, J., Qiu, S., Chen, S., Xiong, C., Liu, H., Wang, J., Zhang, N., Hou, J., He, Q., Nie, Z.:** MALDI-TOF MS imaging of metabolites with a N-(1-Naphthyl) ethylenediamine dihydrochloride matrix and its application to colorectal cancer liver metastasis. *Anal. Chem.*, **87**, 422–430 Available at: <http://pubs.acs.org/doi/10.1021/ac504294s>.(2015).
- Wolfender, J.L., Marti, G., Thomas, A., Bertrand, S.:** Current approaches and challenges for the metabolite profiling of complex natural extracts. *J. Chromatogr. A*, **1382**, 136–164 Available at: <http://dx.doi.org/10.1016/j.chroma.2014.10.091>.(2015).
- Yamamoto, S., Bamba, T., Sano, A., Kodama, Y., Imamura, M., Obata, A., Fukusaki, E.:** Metabolite profiling of soy sauce using gas chromatography with time-of-flight mass spectrometry and analysis of correlation with quantitative descriptive analysis. *J. Biosci. Bioeng.*, **114**, 170–175 Available at: <http://dx.doi.org/10.1016/j.jbiosc.2012.03.023>.(2012).
- Yamana, T., Taniguchi, M., Nakahara, T., Ito, Y., Okochi, N., Putri, S.P., Fukusaki, E.:** Component profiling of soy-sauce-like seasoning produced from different raw materials. *Metabolites*, **10** (2020).
- Yasumatsu, K., Moritaka, S.:** Fatty acid compositions of rice lipid and their changes during storage. *Agric. Biol. Chem.*, **28**, 257–264 (1964).
- Yoshizaki, Y., Yamato, H., Takamine, K., Tamaki, H., Ito, K., Sameshima, Y.:** Analysis of volatile compounds in *shochu koji*, *sake koji*, and steamed rice by gas chromatography-mass spectrometry. *J.Inst.Brew.*, **116**, 49–55 Available at: <https://doi.org/10.1002/j.2050-0416.2010.tb00397.x>.(2010).
- Zaima, N., Yoshimura, Y., Kawamura, Y., Moriyama, T.:** Distribution of lysophosphatidylcholine in the endosperm of *Oryza sativa* rice. *Rapid Commun. Mass Spectrom.*, **28**, 1515–1520 (2014).

## List of Publications

### Original papers

Wisman, A. P., Tamada, Y., Hirohata, S., Gomi, K., Fukusaki, E., & Shimma, S. (2020). Mapping *haze-komi* on rice *koji* grains using  $\beta$ -glucuronidase expressing *Aspergillus oryzae* and mass spectrometry imaging. *Journal of bioscience and bioengineering*, 129(3), 296–301. <https://doi.org/10.1016/j.jbiosc.2019.09.016>

Wisman, A. P., Tamada, Y., Hirohata, S., Fukusaki, E., & Shimma, S. (2020). Metabolic visualization reveals the distinct distribution of sugars and amino acids in rice *koji*. *Mass Spectrometry*, 9(1), A0089. <https://doi.org/10.5702/massspectrometry.A0089>

### Conference list

- 1) Adinda Putri Wisman, Eiichiro Fukusaki, Shuichi Shimma. Non-targeted metabolomics of rice *koji* with MALDI-IMS. International BMS Symposium (2016) – Poster and oral presentation.
- 2) Adinda Putri Wisman, Eiichiro Fukusaki, Shuichi Shimma. Non-targeted Metabolomics of Rice *Koji* with MALDI-IMS. 65<sup>th</sup> Mass Spectrometry Society of Japan Annual Meeting (2017) – Poster presentation.
- 3) Adinda Putri Wisman, Eiichiro Fukusaki, Shuichi Shimma. Visualizing metabolites in rice *koji* using MALDI imaging mass spectrometry. 11<sup>th</sup> Metabolome Symposium (2017) – Poster presentation.
- 4) Adinda Putri Wisman, Eiichiro Fukusaki, Shuichi Shimma. Visualizing metabolites in rice *koji* using MALDI imaging mass spectrometry. Japan Society for Bioscience, Biotechnology, and Agrochemistry Annual Meeting (2018) – Oral presentation.
- 5) Adinda Putri Wisman, Yoshihiro Tamada, Takahiro Akashi, Katsuya Gomi, Eiichiro Fukusaki, Shuichi Shimma. Visualizing metabolites in rice *koji* using MALDI imaging mass spectrometry. 70<sup>th</sup> Society for Biotechnology Japan Annual Meeting (2018) – Oral presentation.
- 6) Adinda Putri Wisman, Yoshihiro Tamada, Takahiro Akashi, Katsuya Gomi, Eiichiro Fukusaki, Shuichi Shimma. Metabolites mapping of rice *koji*. 12<sup>th</sup> Metabolome Symposium (2018) – Poster presentation.

- 7) Adinda Putri Wisman, Yoshihiro Tamada, Shuji Hirohata, Katsuya Gomi, Eiichiro Fukusaki, Shuichi Shimma. Mapping *hazekomi* on rice *koji* grains using  $\beta$ -glucuronidase expressing *Aspergillus oryzae* and mass spectrometry imaging. Society for Biotechnology Japan Annual Meeting (2019) – Oral presentation.
- 8) Adinda Putri Wisman, Yoshihiro Tamada, Shuji Hirohata, Katsuya Gomi, Eiichiro Fukusaki, Shuichi Shimma. Mapping *hazekomi* on rice *koji* grains using  $\beta$ -glucuronidase expressing *Aspergillus oryzae* and mass spectrometry imaging. 8<sup>th</sup> Asia-Oceania Mass Spectrometry Conference (2020) – Poster presentation.

## Appendices

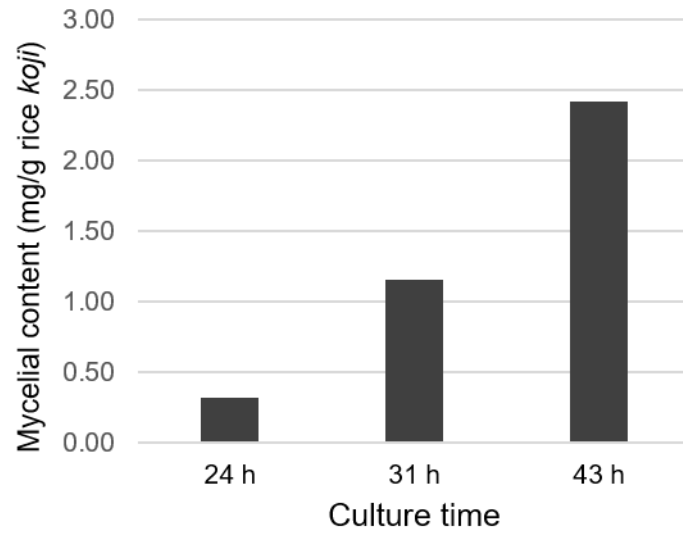


**Figure S1. Mycelial content estimate of GUS rice koji at 24-, 31-, and 43h**

**Table S1. MS-DIAL parameter**

<b>Data type</b>	
Data type	Centroid
Ion mode	Positive
Accuracy type	IsNominal
#Data collection parameters	
Retention time begin	4
Retention time end	25
Mass range begin	85
Mass range end	500
<b>Peak detection parameters</b>	
Smoothing method	Linear Weighted Moving Average
Smoothing level	5
Average peak width	20
Minimum peak height	1000
Mass slice width	0.5
Mass accuracy	0.5
<b>MS1Dec parameters</b>	
Sigma window value	1
Amplitude cut off	200
<b>Identification</b>	
MSP file	GCMS DB_InertCap 5MS-NP_GLscience-VS2.msp
Retention type	RI
RI compound	Alkanes
Retention time tolerance	0.5
Retention index tolerance	10
EI similarity library tolerance	70
Identification score cut off	70
Use retention information for scoring	TRUE
<b>Alignment parameters setting</b>	
Retention index tolerance	10
Retention time tolerance	0.075
EI similarity tolerance	70
Retention time factor	0.5
EI similarity factor	0.5
Gap filling by compulsion	TRUE
<b>Filtering setting</b>	
Peak count filter	0

Remove feature based on peak height fold-change	TRUE
Sample max / blank average	5
Sample average / blank average	5
Keep identified and annotated metabolites	TRUE
Keep removable features and assign the tag for checking	TRUE

**Table S2. A list of tentatively annotated metabolites from GC-MS analysis**

<b>Metabolite name</b>	<b>Retention time (min)</b>	<b>Retention index</b>	<b>Quant mass</b>
Lactic acid	5.06	1064.64	147
Alanine	5.54	1107.71	116
Ketovaline	5.61	1114.31	89
Leucine	6.10	1158.87	86
Valine	6.79	1223.93	144
Glyceraldehyde	6.82	1227.00	147
Urea	6.92	1236.83	189
Serine	7.19	1263.55	116
2-Aminoethanol	7.31	1276.18	174
Glycerol	7.38	1282.88	147
Nicotinic acid	7.50	1294.54	131
Isoleucine	7.56	1301.02	158
Threonine	7.57	1301.71	117
Proline	7.62	1306.82	142
Glycine	7.71	1316.89	147
Uracil	8.00	1347.12	241
Fumaric acid	8.01	1348.62	245
Malic acid	9.35	1498.06	147
Threitol	9.50	1515.49	147
Meso erythritol	9.57	1524.58	147
Aspartic acid	9.63	1531.58	232
Pyroglutamic acid	9.65	1534.74	156
GABA	9.72	1542.33	174
3-Hydroxy-3-methylglutarate	10.30	1614.69	147
Hypotaurine	10.32	1616.69	188
Glutamic acid	10.42	1630.08	246
4-Hydroxybenzoic acid	10.47	1636.32	267
4-Hydroxyphenylacetic acid	10.52	1642.43	117
Phenylalanine	10.52	1643.07	218
Asparagine	10.84	1683.96	116
Arabinose	10.86	1686.03	103
Ribose	10.97	1701.18	103
1,6-Anhydroglucose	11.17	1727.33	260
Xylitol	11.21	1733.86	103
Arabitol	11.31	1746.73	103
Putrescine	11.39	1757.93	174
Glutamine	11.60	1787.22	156

Hypoxanthine	11.84	1820.89	265
3,4-Dihydroxybenzoate	11.93	1833.72	193
Isocitric acid/Citric acid	11.98	1840.27	273
Myristic acid	12.05	1850.33	117
Sorbose	12.43	1905.26	103
Glucono-1,5-lactone	12.47	1911.76	129
Fructose	12.50	1915.81	103
Glucose	12.64	1937.33	160
Tyrosine	12.80	1960.78	280
Mannitol	12.86	1970.09	205
Sorbitol	12.90	1976.42	147
Gluconic acid	13.34	2044.19	147
Inositol	13.90	2133.14	217
Tryptophan	14.41	2219.02	218
Uridine	15.87	2480.74	217
Sucrose	17.02	2705.53	361
Lactose	17.38	2781.09	204
Trehalose	17.57	2820.02	361
Lactitol	17.67	2842.32	361
Maltose	17.71	2850.59	361
Gentiobiose	17.90	2891.11	204
Melibiose	18.17	2953.01	361
Raffinose	20.98	3505.61	204
Maltotriose	22.36	3688.30	204
Panose	23.30	3790.39	204

**Table S3. A list of detected metabolites from LC-MS analysis**

<b>Metabolite name</b>	<b>Precursor ion</b>	<b>Product ion</b>	<b>Retention time (min)</b>
Serine	106.10	60.10	2.19
Valine	118.10	72.05	1.69
Threonine	120.10	74.00	1.89
Cysteine	122.05	59.00	2.60
Isoleucine	132.10	86.15	1.78
Leucine	132.10	86.15	3.34
Asparagine	133.10	74.05	1.70
Aspartic acid	132.20	74.10	2.39
Glutamine	147.10	84.10	2.47
Lysine	147.10	84.10	5.83
Glutamic acid	148.10	84.10	5.84
Methionine	150.10	56.10	4.51
Histidine	156.10	110.10	1.45
Phenylalanine	166.10	120.10	2.42
Arginine	175.10	70.10	1.82
Tyrosine	182.10	136.00	2.33
Tryptophan	205.10	188.15	2.27
Alanine	90.10	44.10	4.04
Proline	116.10	70.10	1.31
Glycine	76.20	29.90	3.26
Ornithine	133.10	70.10	3.35
Spermine	203.15	112.20	1.69
Spermidine	146.45	72.15	2.05
Agmatine	131.40	72.10	1.78
Putrescine	89.25	72.20	3.13
Cadaverine	103.10	86.05	4.04
Betaine	118.10	58.10	1.27
N,N-dimethylglycine	104.05	58.10	1.25
GABA	104.05	87.10	3.23
Hypotaurine	110.15	92.10	3.71

**Table S4. Data matrix from GC-MS and LC-MS analyses used for PCA**

<b>Metabolite name</b>	<b>SR1</b>	<b>SR2</b>	<b>SR3</b>	<b>24A</b>	<b>24B</b>	<b>24C</b>	<b>31A</b>	<b>31B</b>	<b>31C</b>	<b>43A</b>	<b>43B</b>	<b>43C</b>
Serine	0.3866	0.3277	0.4588	0.1732	0.5871	0.5139	1.1755	1.0466	0.8659	0.7687	1.1504	1.1361
Valine	0.0464	0.0335	0.0482	0.9858	0.8802	0.8781	2.2074	1.8275	1.7690	1.3983	1.4860	1.3526
Threonine	0.0189	0.0099	0.0190	0.1793	0.1471	0.1731	0.4309	0.3611	0.3625	0.7515	0.7539	0.6509
Cysteine	0.0052	0.0034	0.0026	0.0244	0.0270	0.0260	0.0130	0.0161	0.0163	0.0070	0.0068	0.0069
Isoleucine	0.0185	0.0243	0.0424	0.6739	0.5421	0.6336	1.6600	1.4130	1.2535	0.9134	0.9467	0.8764
Leucine	0.0228	0.0132	0.0225	1.1277	1.1482	1.1348	2.0943	1.6117	1.6880	0.9638	0.9950	0.5884
Asparagine	0.0797	0.0550	0.0780	0.1857	0.1702	0.1836	0.4341	0.3354	0.3336	0.3121	0.2570	0.2539
Aspartic acid	0.3192	0.2421	0.2898	0.3241	0.3457	0.4244	0.7883	0.7448	0.6882	1.2429	1.2495	1.1289
Glutamine	0.1826	0.1522	0.1560	3.6266	3.6873	4.0032	19.1860	14.7433	13.6091	29.9938	29.4802	21.9610
Lysine	0.0469	0.0434	0.0754	1.2529	1.1478	1.3665	3.4415	2.6478	3.6221	4.7125	4.6757	4.0375
Glutamic acid	0.0000	0.0000	0.0000	0.0354	0.0246	0.0394	0.0692	0.0473	0.0681	0.0906	0.0799	0.0751
Methionine	0.0036	0.0041	0.0059	0.1548	0.1447	0.1684	0.3337	0.2349	0.2383	0.2028	0.2143	0.1507
Histidine	0.0354	0.0360	0.0296	0.8016	0.6158	0.7223	2.0011	2.0506	1.7974	3.3345	3.2127	2.9506
Phenylalanine	0.0621	0.0482	0.0944	1.8899	2.2511	2.1917	3.9863	3.4426	2.9025	1.8074	1.6901	1.4821
Arginine	0.1458	0.1290	0.1627	10.7400	9.4577	9.9690	21.8319	20.1564	18.0811	20.7806	19.7704	18.5951
Tyrosine	0.0191	0.0133	0.0212	0.6388	0.7683	0.7218	2.2934	1.9284	1.8781	2.4393	2.4051	1.9324
Tryptophan	0.0067	0.0109	0.0108	0.2151	0.2341	0.2515	0.7670	0.5536	0.5907	0.6665	0.7971	0.5555
Alanine	0.0421	0.0364	0.0734	0.5531	0.4845	0.5306	1.4767	1.0537	1.1355	2.8553	2.7839	1.7692
Proline	0.0659	0.0583	0.0825	1.1582	0.9223	0.9569	2.6623	2.3818	2.0756	3.3092	3.2450	2.8876
Glycine	0.0062	0.0061	0.0115	0.0391	0.0319	0.0389	0.0968	0.0721	0.0756	0.1217	0.1325	0.0778
Citrulline	0.0129	0.0099	0.0419	0.0057	0.0103	0.0149	0.0405	0.0189	0.0267	0.1066	0.0717	0.0319
Ornithine	0.0294	0.0278	0.0563	0.2962	0.2279	0.2802	1.2833	0.9857	1.0662	7.9907	7.8514	4.5276
Spermine	0.2485	0.0699	0.0419	0.2452	0.0769	0.0465	0.4010	0.1383	0.0905	0.3485	0.1566	0.0933
Spermidine	0.0448	0.0163	0.0765	0.0404	0.0235	0.0145	0.2246	0.1492	0.1033	0.1550	0.1563	0.0837

Agmatine	0.0696	0.0379	0.0491	0.4014	0.3132	0.3224	13.2390	13.3234	9.6891	6.1444	6.6990	5.9304
Putrescine	0.0099	0.0278	0.0227	0.9900	0.9770	0.9886	2.4776	2.1790	2.0250	3.9237	4.2999	3.0257
Cadaverine	0.0000	0.0000	0.0000	0.0000	0.0000	0.0000	0.0351	0.0329	0.0339	0.0807	0.0905	0.0637
Betaine	0.0797	0.1622	0.0851	5.7455	4.8071	4.8999	15.3158	14.7423	13.6499	24.5724	24.8596	20.7902
N,N-dimethylglycine	0.6579	0.5973	0.7015	2.9251	2.7138	2.6728	3.5981	3.3490	2.7036	2.5168	2.5674	2.3212
GABA	0.0279	0.0229	0.0248	1.2021	1.1782	1.2520	6.2567	4.9240	5.1481	11.3399	11.3894	6.8113
Hypotaurine	0.0000	0.0000	0.0000	0.0158	0.0211	0.0196	0.0654	0.0456	0.0501	0.0684	0.0684	0.0495
Lactic acid	0.0248	0.0245	0.0275	0.0155	0.0174	0.0216	0.0137	0.0210	0.0214	0.0159	0.0142	0.0157
Ketovalline	0.0003	0.0003	0.0002	0.0043	0.0046	0.0045	0.0013	0.0016	0.0014	0.0006	0.0004	0.0003
Glyceraldehyde	0.0004	0.0004	0.0006	0.0021	0.0030	0.0025	0.0039	0.0037	0.0035	0.0147	0.0181	0.0151
Urea	0.0011	0.0017	0.0016	0.0010	0.0012	0.0010	0.0011	0.0018	0.0013	0.0014	0.0014	0.0011
2-Aminoethanol	0.0015	0.0015	0.0016	0.0200	0.0213	0.0208	0.0338	0.0334	0.0340	0.0377	0.0359	0.0350
Glycerol	0.0400	0.0476	0.0459	0.8688	0.8982	0.9241	3.7407	3.9031	3.8581	6.3714	6.3314	6.1400
Nicotinic acid	0.0008	0.0009	0.0006	0.0011	0.0012	0.0012	0.0014	0.0013	0.0010	0.0010	0.0010	0.0012
Uracil	0.0003	0.0003	0.0003	0.0005	0.0006	0.0004	0.0015	0.0017	0.0014	0.0052	0.0050	0.0047
Fumaric acid	0.0016	0.0016	0.0019	0.0028	0.0033	0.0033	0.0025	0.0029	0.0027	0.0036	0.0042	0.0038
Malic acid	0.0116	0.0126	0.0114	0.0355	0.0376	0.0399	0.0288	0.0296	0.0298	0.0342	0.0339	0.0361
Threitol	0.0006	0.0007	0.0006	0.0004	0.0008	0.0011	0.0043	0.0051	0.0049	0.0342	0.0319	0.0321
Meso erythritol	0.0011	0.0012	0.0009	0.0286	0.0306	0.0309	0.2889	0.2931	0.2919	2.1752	2.1104	2.0765
Pyroglutamic acid	0.0064	0.0075	0.0076	0.0157	0.0185	0.0202	0.0333	0.0326	0.0351	0.0433	0.0439	0.0551
3-Hydroxy-3-methylglutarate	0.0005	0.0006	0.0006	0.0030	0.0032	0.0034	0.0085	0.0095	0.0099	0.0304	0.0283	0.0284
4-Hydroxybenzoic acid	0.0002	0.0003	0.0002	0.0018	0.0018	0.0019	0.0040	0.0045	0.0046	0.0022	0.0020	0.0021

4-Hydroxyphenylacetic acid	0.0010	0.0010	0.0015	0.0011	0.0014	0.0020	0.0014	0.0018	0.0018	0.0013	0.0009	0.0018
Arabinose	0.0010	0.0011	0.0010	0.0036	0.0038	0.0038	0.0180	0.0196	0.0182	0.0553	0.0531	0.0537
Ribose	0.0014	0.0019	0.0017	0.0307	0.0327	0.0343	0.0777	0.0810	0.0799	0.0845	0.0837	0.0838
1,6-Anhydroglucose	0.0002	0.0002	0.0001	0.0005	0.0003	0.0006	0.0012	0.0013	0.0012	0.0015	0.0014	0.0010
Xylitol	0.0005	0.0003	0.0003	0.0008	0.0005	0.0007	0.0027	0.0026	0.0023	0.0105	0.0101	0.0098
Arabitol	0.0002	0.0000	0.0000	0.0540	0.0577	0.0593	0.3637	0.3860	0.3752	0.9903	0.9422	0.9490
Hypoxanthine	0.0002	0.0002	0.0001	0.0024	0.0023	0.0026	0.0051	0.0052	0.0053	0.0077	0.0067	0.0075
3,4-Dihydroxybenzoate	0.0003	0.0003	0.0002	0.0007	0.0002	0.0010	0.0025	0.0027	0.0023	0.0038	0.0034	0.0035
Isocitric/Citric acid	0.0104	0.0114	0.0129	0.1018	0.1084	0.1112	0.1757	0.1895	0.1804	0.0899	0.0913	0.0942
Myristic acid	0.0059	0.0061	0.0064	0.0066	0.0063	0.0065	0.0064	0.0074	0.0071	0.0061	0.0061	0.0059
Sorbose	0.0076	0.0087	0.0085	0.0183	0.0195	0.0205	0.0242	0.0261	0.0254	0.0348	0.0356	0.0351
Glucono-1,5-lactone	0.0011	0.0011	0.0019	0.0031	0.0031	0.0043	0.0040	0.0052	0.0052	0.0044	0.0051	0.0052
Fructose	0.0048	0.0047	0.0050	0.0107	0.0109	0.0114	0.0128	0.0133	0.0114	0.0121	0.0134	0.0112
Glucose	0.0116	0.0149	0.0154	2.9755	2.9297	2.9569	9.3166	9.6111	9.2322	13.0539	13.2633	12.8705
Mannitol	0.0007	0.0008	0.0009	0.3301	0.3477	0.3504	0.5755	0.5904	0.5726	1.0966	1.0330	1.0083
Sorbitol	0.0011	0.0011	0.0008	0.3062	0.3228	0.3249	0.0110	0.0101	0.0095	0.0846	0.0799	0.0810
Gluconic acid	0.0017	0.0012	0.0013	0.0162	0.0162	0.0174	0.0331	0.0318	0.0329	0.0426	0.0404	0.0460
Inositol	0.0010	0.0012	0.0010	0.0045	0.0044	0.0045	0.0102	0.0111	0.0116	0.0167	0.0163	0.0176
Uridine	0.0007	0.0006	0.0008	0.0016	0.0019	0.0025	0.0028	0.0034	0.0035	0.0037	0.0039	0.0045
Sucrose	0.0327	0.0368	0.0372	0.0124	0.0143	0.0126	0.0103	0.0104	0.0105	0.0098	0.0090	0.0085
Lactose	0.0006	0.0011	0.0008	0.2718	0.2996	0.2902	0.1612	0.1660	0.1562	0.0911	0.0898	0.0916
Trehalose	0.0066	0.0093	0.0109	6.8170	6.6362	7.2176	4.4375	4.3221	4.3488	3.4522	3.3043	3.3004

Lactitol	0.0022	0.0022	0.0028	2.4948	2.4203	0.0300	0.2656	0.2835	0.2774	0.9008	0.9023	0.8732
Maltose	0.0022	0.0022	0.0026	2.4760	2.4019	2.5938	1.1928	1.1846	1.1715	0.5404	0.5328	0.5145
Gentiobiose	0.0008	0.0010	0.0009	0.0018	0.0032	0.0020	0.0103	0.0121	0.0113	0.0418	0.0399	0.0363
Melibiose	0.0008	0.0012	0.0016	1.2030	1.3081	1.3025	3.0602	3.2361	3.1312	4.8261	4.8076	4.5886
Raffinose	0.0008	0.0010	0.0010	0.0207	0.0226	0.0285	0.0080	0.0093	0.0110	0.0124	0.0133	0.0129
Maltotriose	0.0022	0.0036	0.0039	0.2984	0.3063	0.3326	0.1173	0.1209	0.1281	0.1599	0.1613	0.1711
Panose	0.0008	0.0011	0.0011	0.0624	0.0663	0.0707	0.0971	0.1005	0.1013	0.0700	0.0705	0.0765

**Table S5. Significance of each metabolites change detected from GC-MS and LC-MS analysis. Bold font with red background is  $p < 0.01$ . Bold font is  $p < 0.05$ .**

<b>Metabolite name</b>	<b>SR vs 24h</b>	<b>SR vs 31h</b>	<b>SR vs 43h</b>	<b>24h vs 31h</b>	<b>24h vs 43h</b>	<b>31h vs 43h</b>
1,6-Anhydroglucose	< <b>0.05</b>	< <b>0.01</b>	< <b>0.01</b>	< <b>0.01</b>	< <b>0.01</b>	> 0.05
Arabionose	< <b>0.01</b>	< <b>0.01</b>	< <b>0.01</b>	< <b>0.01</b>	< <b>0.01</b>	< <b>0.01</b>
Fructose	< <b>0.01</b>	< <b>0.01</b>	< <b>0.01</b>	> 0.05	> 0.05	> 0.05
Gentiobiose	> 0.05	< <b>0.01</b>	< <b>0.01</b>	< <b>0.01</b>	< <b>0.01</b>	< <b>0.01</b>
Glucose	< <b>0.01</b>	< <b>0.01</b>	< <b>0.01</b>	< <b>0.01</b>	< <b>0.01</b>	< <b>0.01</b>
Glyceraldehyde	< <b>0.01</b>	< <b>0.01</b>	< <b>0.01</b>	< <b>0.01</b>	< <b>0.01</b>	< <b>0.01</b>
Lactose	< <b>0.01</b>	< <b>0.01</b>	< <b>0.01</b>	< <b>0.01</b>	< <b>0.01</b>	< <b>0.01</b>
Maltose	< <b>0.01</b>	< <b>0.01</b>	< <b>0.01</b>	< <b>0.01</b>	< <b>0.01</b>	< <b>0.01</b>
Maltotriose	< <b>0.01</b>	< <b>0.01</b>	< <b>0.01</b>	< <b>0.01</b>	< <b>0.01</b>	< <b>0.01</b>
Melibiose	< <b>0.01</b>	< <b>0.01</b>	< <b>0.01</b>	< <b>0.01</b>	< <b>0.01</b>	< <b>0.01</b>
Panose	< <b>0.01</b>	< <b>0.01</b>	< <b>0.01</b>	< <b>0.01</b>	> 0.05	< <b>0.01</b>
Raffinose	< <b>0.01</b>	< <b>0.01</b>	< <b>0.01</b>	< <b>0.01</b>	< <b>0.05</b>	< <b>0.05</b>
Ribose	< <b>0.01</b>	< <b>0.01</b>	< <b>0.01</b>	< <b>0.01</b>	< <b>0.01</b>	< <b>0.05</b>
Sorbose	< <b>0.01</b>	< <b>0.01</b>	< <b>0.01</b>	< <b>0.01</b>	< <b>0.01</b>	< <b>0.01</b>
Sucrose	< <b>0.01</b>	< <b>0.01</b>	< <b>0.01</b>	< <b>0.05</b>	< <b>0.01</b>	> 0.05
Trehalose	< <b>0.01</b>	< <b>0.01</b>	< <b>0.01</b>	< <b>0.01</b>	< <b>0.01</b>	< <b>0.01</b>
Arabitol	> 0.05	> 0.05	> 0.05	< <b>0.01</b>	< <b>0.01</b>	< <b>0.01</b>
Glycerol	< <b>0.01</b>	< <b>0.01</b>	< <b>0.01</b>	< <b>0.01</b>	< <b>0.01</b>	< <b>0.01</b>
Inositol	< <b>0.01</b>	< <b>0.01</b>	< <b>0.01</b>	< <b>0.01</b>	< <b>0.01</b>	< <b>0.01</b>
Lactitol	> 0.05	< <b>0.01</b>	< <b>0.01</b>	> 0.05	> 0.05	< <b>0.01</b>
Mannitol	< <b>0.01</b>	< <b>0.01</b>	< <b>0.01</b>	< <b>0.01</b>	< <b>0.01</b>	< <b>0.01</b>
Meso erythritol	< <b>0.01</b>	< <b>0.01</b>	< <b>0.01</b>	< <b>0.01</b>	< <b>0.01</b>	< <b>0.01</b>

Sorbitol	< 0.01	< 0.01	< 0.01	< 0.01	< 0.01	< 0.01
Threitol	> 0.05	< 0.01	< 0.01	< 0.01	< 0.01	< 0.01
Xylitol	> 0.05	< 0.01	< 0.01	< 0.01	< 0.01	< 0.01
Alanine	< 0.01	< 0.05	< 0.05	< 0.05	< 0.05	< 0.05
Arginine	< 0.01	< 0.01	< 0.01	< 0.01	< 0.01	> 0.05
Asparagine	< 0.01	< 0.01	< 0.01	< 0.05	< 0.01	> 0.05
Aspartic acid	> 0.05	< 0.01	< 0.01	< 0.01	< 0.01	< 0.01
Cysteine	< 0.01	< 0.01	> 0.05	< 0.01	< 0.01	< 0.05
GABA	< 0.01	< 0.01	< 0.05	< 0.01	< 0.05	< 0.05
Glutamic acid	< 0.05	< 0.05	< 0.01	< 0.05	< 0.01	> 0.05
Glutamine	< 0.01	< 0.05	< 0.01	< 0.05	< 0.05	< 0.05
Glycine	< 0.01	< 0.01	< 0.05	< 0.01	< 0.05	> 0.05
Histidine	< 0.01	< 0.01	< 0.01	< 0.01	< 0.01	< 0.01
Isoleucine	< 0.01	< 0.01	< 0.01	< 0.01	< 0.01	< 0.05
Leucine	< 0.01	< 0.01	< 0.05	< 0.05	> 0.05	< 0.01
Lysine	< 0.01	< 0.01	< 0.01	< 0.01	< 0.01	< 0.05
Methionine	< 0.01	< 0.05	< 0.05	< 0.05	> 0.05	> 0.05
Ornithine	< 0.01	< 0.01	< 0.05	< 0.01	< 0.05	< 0.05
Phenylalanine	< 0.01	< 0.01	< 0.01	< 0.05	< 0.05	< 0.01
Proline	< 0.01	< 0.01	< 0.01	< 0.01	< 0.01	< 0.05
Serine	> 0.05	< 0.01	< 0.01	< 0.05	< 0.05	> 0.05
Threonine	< 0.01	< 0.01	< 0.01	< 0.01	< 0.01	< 0.01
Tryptophan	< 0.01	< 0.05	< 0.05	< 0.05	< 0.05	> 0.05
Tyrosine	< 0.01	< 0.01	< 0.01	< 0.01	< 0.01	> 0.05
Valine	< 0.01	< 0.01	< 0.01	< 0.01	< 0.01	< 0.05
4-Hydroxybenzoic acid	< 0.01	< 0.01	< 0.01	< 0.01	< 0.05	< 0.01

4-Hydroxyphenylacetic acid	> 0.05	> 0.05	> 0.05	> 0.05	> 0.05	> 0.05
Fumaric acid	< 0.01	< 0.01	< 0.01	> 0.05	< 0.05	< 0.01
Gluconic acid	< 0.01	< 0.01	< 0.01	< 0.01	< 0.01	< 0.01
Isocitric/Citric acid	< 0.01	< 0.01	< 0.01	< 0.01	< 0.01	< 0.01
Lactic acid	< 0.05	> 0.05	< 0.01	> 0.05	> 0.05	> 0.05
Malic acid	< 0.01	< 0.01	< 0.01	< 0.01	> 0.05	< 0.01
Myristic acid	> 0.05	> 0.05	> 0.05	> 0.05	< 0.05	> 0.05
Nicotinic acid	< 0.01	< 0.05	< 0.05	> 0.05	> 0.05	> 0.05
Pyroglutamic acid	< 0.01	< 0.01	< 0.01	< 0.01	< 0.01	< 0.05
Agmatine	< 0.01	< 0.01	< 0.01	< 0.01	< 0.01	< 0.01
Putrescine	< 0.01	< 0.01	< 0.01	< 0.01	< 0.05	< 0.05
Spermidine	> 0.05	< 0.05	< 0.05	< 0.05	< 0.05	> 0.05
Spermine	> 0.05	> 0.05	> 0.05	> 0.05	> 0.05	> 0.05
2-Aminoethanol	< 0.01	< 0.01	< 0.01	< 0.01	< 0.01	< 0.05
3,4-Dihydroxybenzoate	> 0.05	< 0.01	< 0.01	< 0.01	< 0.01	< 0.01
3-Hydroxy-3-methylglutarate	< 0.01	< 0.01	< 0.01	< 0.01	< 0.01	< 0.01
Betaine	< 0.01	< 0.01	< 0.01	< 0.01	< 0.01	< 0.01
Cadaverine	> 0.05	< 0.01	< 0.01	< 0.01	< 0.01	< 0.05
Glucono-1,5-lactone	< 0.01	< 0.01	< 0.01	> 0.05	< 0.05	> 0.05
Hypotaurine	< 0.01	< 0.05	< 0.01	< 0.01	< 0.01	> 0.05
Hypoxanthine	< 0.01	< 0.01	< 0.01	< 0.01	< 0.01	< 0.01
Ketovaline	< 0.01	< 0.01	> 0.05	< 0.01	< 0.01	< 0.01
N,N-dimethylglycine	< 0.01	< 0.01	< 0.01	> 0.05	< 0.05	> 0.05
Uracil	> 0.05	< 0.01	< 0.01	< 0.01	< 0.01	< 0.01
Urea	> 0.05	> 0.05	> 0.05	> 0.05	> 0.05	> 0.05
Uridine	< 0.05	< 0.01	< 0.01	< 0.05	< 0.01	> 0.05

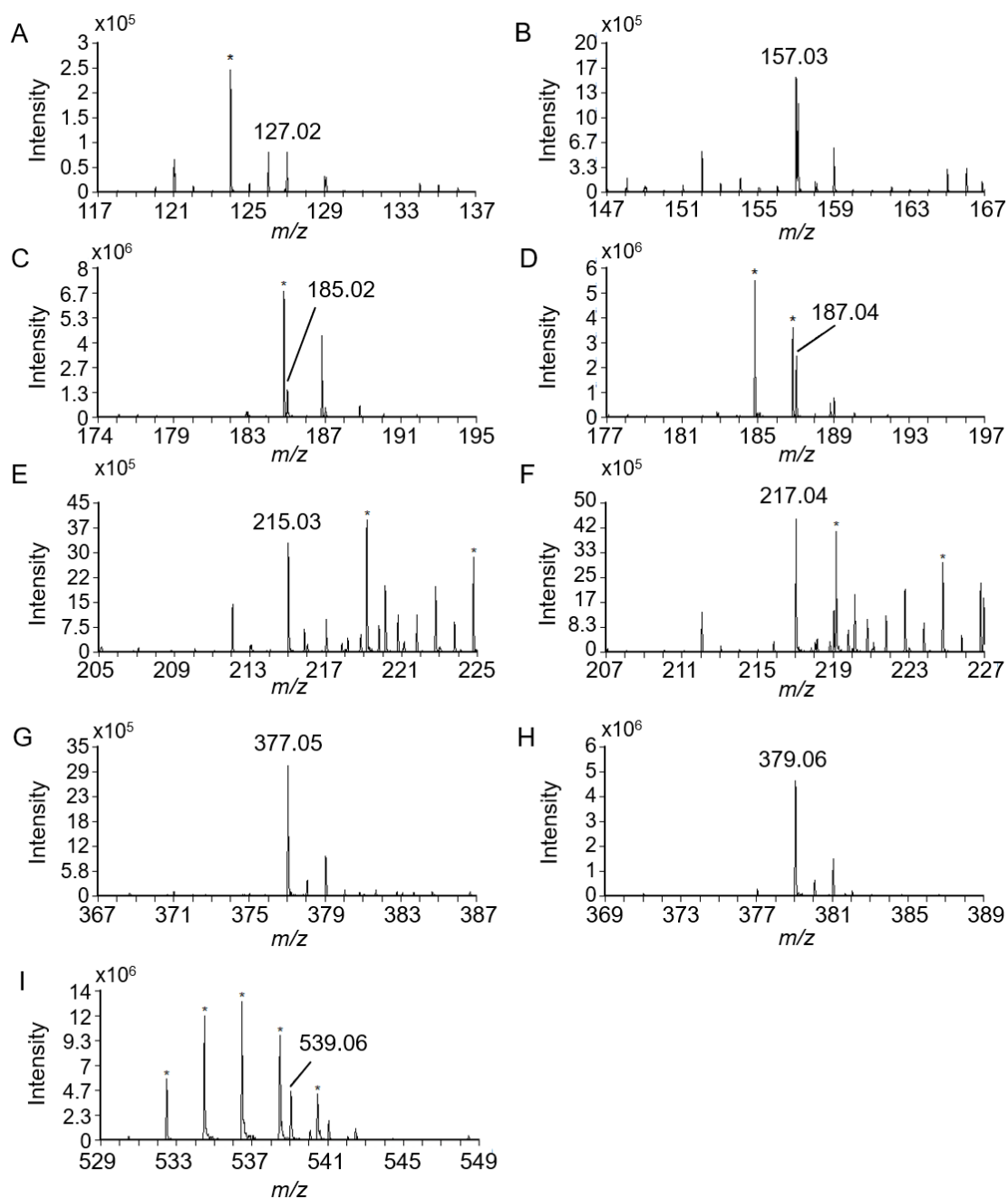


**Figure S2. Mass spectra of detected sugar standards in MSI. (A) Glycerol; (B) meso erythritol and threitol; (C) arabinose and ribose; (D) arabitol and xylitol; (E) fructose, glucose, inositol, and sorbose; (F) mannitol and sorbitol; (G) gentiobiose, lactose, maltose, melibiose, sucrose, and trehalose; (H) lactitol; (I) maltotriose, panose and raffinose. Peaks with asterisk originated from matrix.**

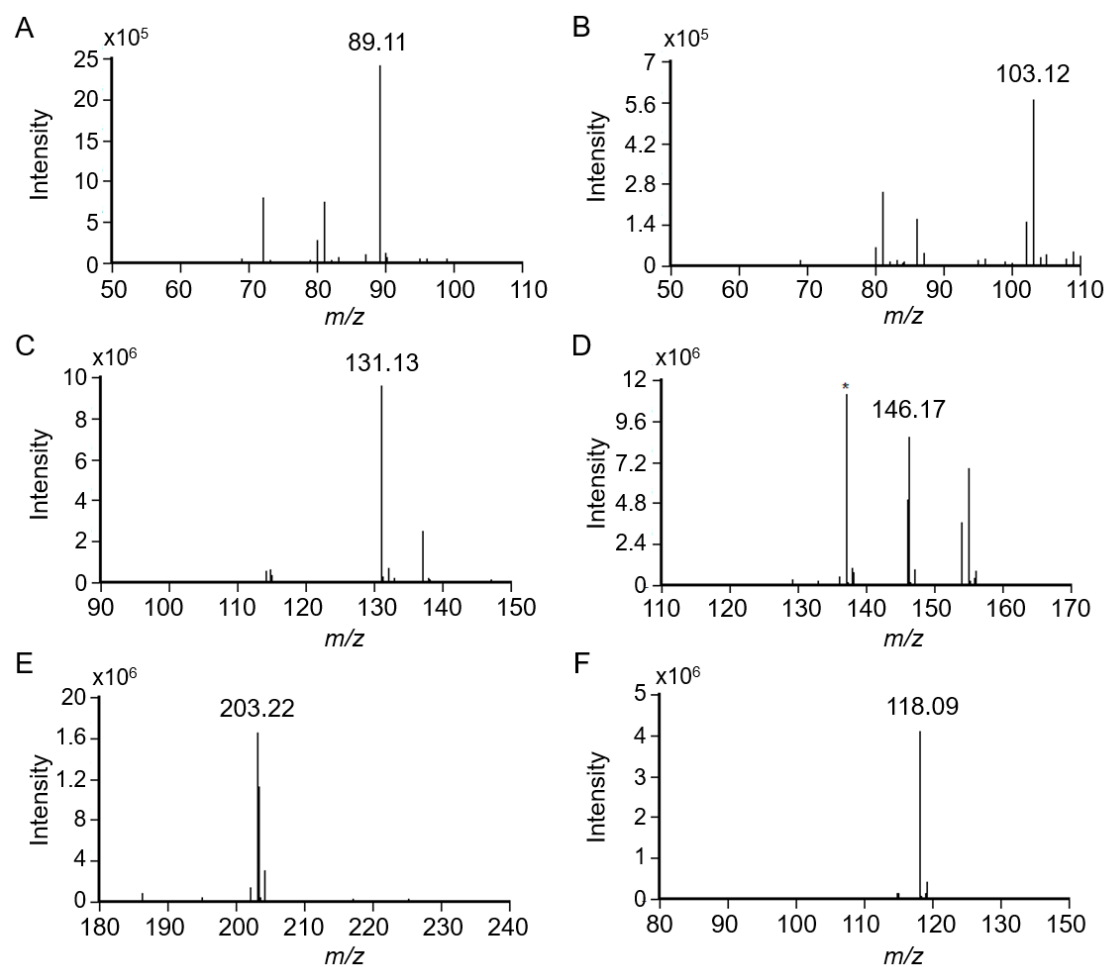


**Figure S3. Mass spectra of detected amine metabolites in MSI. (A) Putrescine; (B) cadaverine; (C) agmatine; (D) spermidine; (E) spermine; (F) betaine. Peaks with asterisk originated from matrix.**

## Acknowledgment

I would like to express my sincere gratitude to Bioresource Engineering laboratory professors, Prof. Eiichiro Fukusaki, Assoc. Prof. Shuichi Shimma, and Assist. Prof. Sastia Prama Putri. Their valuable insights and constructive suggestions have guided me plenty throughout my master and doctoral study. During my worst, their kind patience and understanding motivated me to become a better person. I am also grateful to my co-supervisors Prof. Kazuhito Fujiyama and Prof. Takeharu Nagai for the kind and helpful suggestions to improve my thesis. I would like to give special appreciation to my collaborator from Tohoku University, Prof. Katsuya Gomi, for constructing the GUS *A. oryzae* strain and the suggestions for my paper. I would also like to extend my gratitude to my collaborator from Hakutsuru Brewing Company, Yoshihiro Tamada-san, for providing the samples, additional data, and engaging discussions regarding rice *koji*.

I would like to address all of the staff and lab members in Fukusaki Lab. Special thanks to Taniguchi-san for the helpful assistance and knowledge sharing regarding rice *koji* and *sake* brewery. I also wish to thank the MSI team members, especially Takeo-san, for being not just a lab mate but also a friend. I could not forget my dear lab members, especially Kadar, Moke, Safira, Ploy, and Fitri. Thank you for being there for me and being my moral support. My gratitude also goes for the graduated lab members that still kept in contact with me and wished for my success. I would like to extend a special thanks to my dearest friend, Pijar, for the five years of struggling together for Ph.D. under one roof. You are like my family here in Japan. Finally, I would like to thank my family in Indonesia for the support, encouragement, understanding, and patience. My gratefulness cannot be expressed by words.